AD-A119 494 AEROSPACE CORP EL SEGUNDO CA MATERIALS SCIENCES LAB F/G 7/4
CALIBRATION OF A MASS SPECTROMETER FOR ANALYSIS OF ULTRAMICRO G--ETC(U)
AUG 82 W M GRAVEN, D E GILMARTIN F04701-81-C-0082
UNCLASSIFIED TR-0082(2935-03)-3 SD-TR-82-55 NL

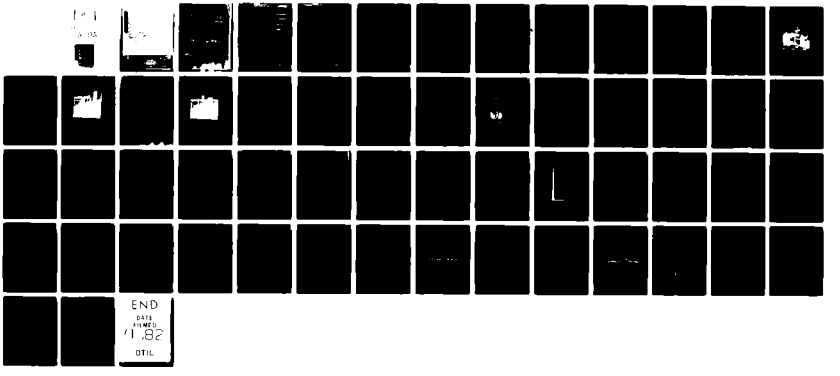

END
DATE FILMED
11-82
DTIC

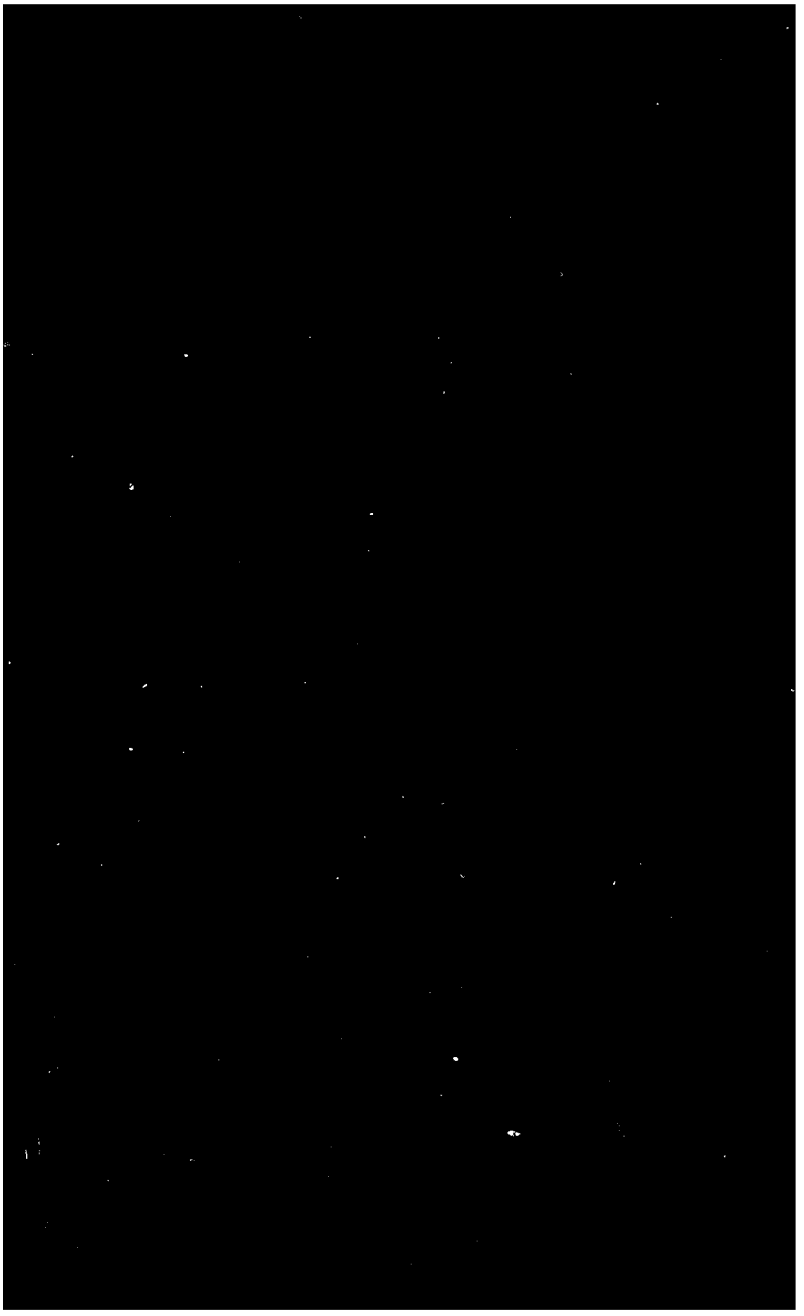

This report was submitted by The Aerospace Corporation, El Segundo, CA 90245, under Contract No. FO4701-82-C-0082 with the Space Systems Division, Air Force Systems Command, P.O. Box 92960, Worldway Postal Center, Los Angeles, CA 90009. It was reviewed and approved for The Aerospace Corporation by W. C. Kelly, Director, Materials Sciences Laboratories. Major John A. Criscuolo, SSD/YEST was the project officer for the Mission-Oriented Investigation and Experimentation (MOIE) Program.

This report has been reviewed by the Public Affairs Office (PAS) and is releasable to the National Technical Information Service (NTIS). At NTIS, it will be available to the general public, including foreign nations.

This technical report has been reviewed and is approved for publication. Publication of this report does not constitute Air Force approval of the report's findings or conclusions. It is published only for the exchange and stimulation of ideas.

John A. Criscuolo

John A. Criscuolo, Major, USAF
Project Officer

James H. Butler

James H. Butler, Colonel, USAF
Director of Space Systems Technology

FOR THE COMMANDER

William J. Ince, Jr., Col, USAF
Deputy for Technology

UNCLASSIFIED

SECURITY CLASSIFICATION OF THIS PAGE (When Data Entered)

REPORT DOCUMENTATION PAGE

READ INSTRUCTIONS BEFORE COMPLETING FORM

1. REPORT NUMBER: SD-TR-82-55	2. GOVT ACCESSION NO.: AD-A119497
3. RECIPIENT'S CATALOG NUMBER:	
4. TITLE (and Subtitle): CALIBRATION OF A MASS SPECTROMETER FOR ANALYSIS OF ULTRAMICRO GAS SAMPLES USING A DYNAMIC METHOD OF ANALYSIS	5. TYPE OF REPORT & PERIOD COVERED:
	6. PERFORMING ORG. REPORT NUMBER: TR-0082(2935-03)-3
7. AUTHOR(s): Wendell M. Graven and Donald E. Gilmartin	8. CONTRACT OR GRANT NUMBER(s): F04701-81-C-0082
9. PERFORMING ORGANIZATION NAME AND ADDRESS: The Aerospace Corporation, El Segundo, Calif. 90245	10. PROGRAM ELEMENT, PROJECT, TASK AREA & WORK UNIT NUMBERS:
11. CONTROLLING OFFICE NAME AND ADDRESS: Space Division, Air Force Systems Command, Los Angeles, Calif. 90009	12. REPORT DATE: 16 August 1982
	13. NUMBER OF PAGES: 53
14. MONITORING AGENCY NAME & ADDRESS (if different from Controlling Office)	15. SECURITY CLASS. (of this report): Unclassified
	15a. DECLASSIFICATION/DOWNGRADING SCHEDULE:

16. DISTRIBUTION STATEMENT (of this Report)

Approved for public release; distribution unlimited

17. DISTRIBUTION STATEMENT (of the abstract entered in Block 20, if different from Report)

18. SUPPLEMENTARY NOTES

19. KEY WORDS (Continue on reverse side if necessary and identify by block number)

Traveling-Wave Tube (TWT)	Ionization Gauge
Residual Gas Analysis	Calibrated Leak
Instrument Calibration	Ultramicro Gas Sample
Mass Spectrometer	Ultrahigh Vacuum

20. ABSTRACT (Continue on reverse side if necessary and identify by block number)

A special-purpose mass spectrometer was allocated to analyze very small amounts of residual gases in electronic devices, principally traveling wave tubes. Because of device-related constraints that made it necessary to transport ultramicro amounts of gas to the analyzer, a dynamic method of analysis was adopted. Using calibrated leak sources, reliable transport and reproducible analyses of ultramicro amounts of gases were demonstrated with seven gases over a four-decade range. For inert gases, the reproducible

DD FORM 1473 (FACSIMILE)

UNCLASSIFIED

SECURITY CLASSIFICATION OF THIS PAGE (When Data Entered)

19. KEY WORDS (Continued)

(10 to THE -11TH POWER)

(ATM/CU CM)

20. ABSTRACT (Continued)

analytical range extended below 10^{-11} atm cm^3. Extensive calibrations were carried out with eight gases by using both the residual gas analyzer and the ionization gauge as detection instruments. These data, as well as the results of residual gas analyses conducted with production-quality traveling wave tubes, have validated the dynamic method of analysis.

CONTENTS

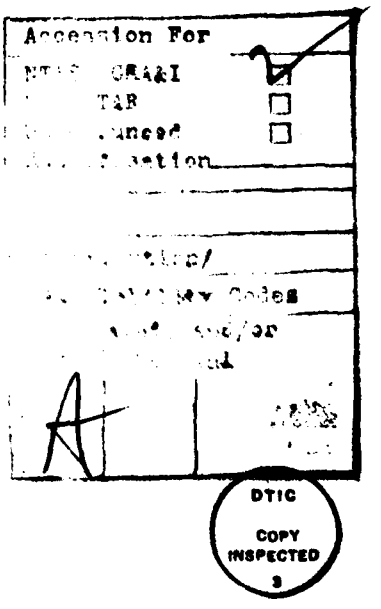

FIGURES

FIGURES (Continued)

TABLES

I. INTRODUCTION

A well-established method of calibrating an analytical mass spectrometer is to introduce a pure gaseous sample and measure the output of the instrument as a function of the pressure of the sample. Usually, the steady-state pressure in the mass spectrometer is measured with an ionization gauge that also must be calibrated. The indicated pressure is called a steady-state pressure because it is established from the combined effects of adsorption, desorption, outgassing of wall surfaces, pumping by hot filaments, and alteration by chemical processes. Therefore, in a vacuum system that is isolated from its primary pump, the indicated pressure may rise or fall with time, and this problem is magnified as the pressure is decreased. For work in the ultrahigh vacuum region, i.e., at pressures lower than 10^{-8} Torr, special techniques are required to calibrate pressure gauges. The use of these gauges for accurate pressure measurements is fraught with problems (Ref. 1). If, in addition to the ultrahigh vacuum conditions, extremely small gas samples are to be measured quantitatively, the difficulties associated with the conventional analytical method are nearly insurmountable. The absolute determination of small amounts of gases by means of a static system is limited to the analysis of the rare gases. Samples of the order of 10^{-8} atm cm^3 can be measured, provided the instrument is calibrated immediately before and after the measurement (Ref. 2).

A unique requirement motivated our exploration of an alternative analytical approach, and its successful application in our calibration efforts is the subject of this report. Our task was to analyze, both qualitatively and quantitatively, the residual gases in microwave amplifier tubes or diodes containing electron guns. The traveling-wave tubes were production hardware of such size and construction that required external adaptation so that their residual gas could be transported to the analytical instrument. The amounts of gases expected were of the order of 10^{-10} to 10^{-8} atm cm^3, which corresponded to pressures of 10^{-9} to 10^{-7} Torr in the devices. Therefore, transfer of the gas to the analytical instrument was practicable provided that the

vacuum system pressure was about 10^{-11} Torr. By introducing the gas to be analyzed directly into the closed ion-source chamber of a mass spectrometer that was being pumped continuously, one could conduct a dynamic analysis before the gas was either pumped away or had an opportunity to interact with the system, other than with the walls of the inlet valve and tubing. With this method, the problems previously cited were minimized. Of course, the method required a mass spectrometer with a sub-second scanning speed so that a sufficient number of complete analyses could be made to quantify the sample before the gas pulse had passed out of the source chamber. Computerized instruments with this capability were available. However, the instrument had to be calibrated by the same dynamic method that was to be used for the residual gas analyses. This report includes the results of rather extensive calibrations with eight gases that were potential denizens of the devices to be analyzed.

II. APPARATUS

All of the calibration measurements were made with a quadrupole mass spectrometer built by Finnigan Corp. A photograph of the instrument is shown in Fig. 1. Although the instrument was custom built to our specifications, it consisted of a Series 3200 mass analyzer and a Series 6110 data-handling system, both from Finnigan's standard GC/MS systems. The available mass range was 1 to 500 amu, but for our purpose only the range of 1 to 50 amu was used. After a 1-h warm-up, mass peak drift was less than ±0.1 amu over an 8-h period. The normal resolution (M/ΔM) was greater than 500; however, resolution could be programmed for nearly constant sensitivity over the mass range that was utilized. The sensitivity of 50 A/Torr at the electron multiplier resulted in a minimum detectable pressure of 1×10^{-14} Torr (nitrogen) with a signal/noise ratio of 2. The use of an offset, continuous dynode Channeltron electron multiplier allowed the manifold to be baked at 400°C. The scan rate was continuously variable down to 0.4 sec/scan for the 1-to-50-amu range that was used.

The interactive data system was built around a Computer Automation central processor with a 16-k, 16-bit word memory. A removable magnetic disc and a tape cartridge facility were available to give a 1200-k, 16-bit word data storage capacity. Although the operational software was designed for GC/MS application, much of it was ideally suited to our dynamic method of analysis. In fact, if we were to have had it developed specifically for our purpose it could not have been much improved.

The custom-designed vacuum system was built to our specifications. It was constructed entirely of metal with ceramic insulation of electrical feedthroughs. Portions of the instrument were enclosed in ovens so that they could be baked at 400°C. The operational pressure of 10^{-11} Torr was achieved with an isolatable ion pump that was supported by a titanium sublimator. The vacuum system had the primary pumping speed of the ion pump, i.e., 220 l/sec, since the sublimator was used only for initial clean-up of the vacuum system. In addition to the ion pump current meter, the system pressure was monitored

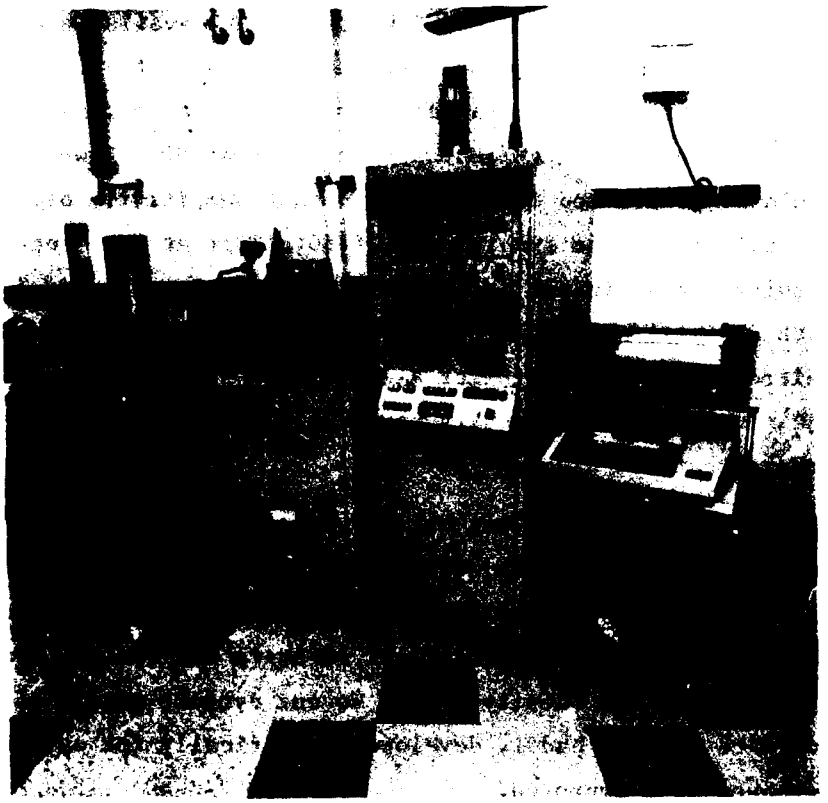

Fig. 1. Equipment Ensemble for Residual Gas Analysis

with a nude ionization gauge that was mounted in the manifold directly above the closed ion source. The output of the Ultek digital ionization gauge controller was fed to an x-y recorder.

With two identical but symmetrically opposed sample inlet systems that were separately ion pumped, gas samples could be introduced through dual ports directly into the closed ion source. A photograph of the sample inlet system is shown in Fig. 2. One inlet system was reserved for calibration purposes and the other was used for residual gas analyses, although the latter was also used for some calibration measurements. A diagram of the calibration and sample inlet systems is shown in Fig. 3. Although the calibration system was a stand-alone vacuum system with its own sorption and ion pumps and ionization gauge, it was intended to be a permanent part of the analytical instrument. A photograph of the calibration system is shown in Fig. 4.

Except for the two sorption pumps, the entire calibration system, including all valves, is bakeable. Although the function of the valves shown is simply to shut off and isolate portions of the vacuum system, our experience has shown that the Granville-Phillips variable leak valves are most suitable for ultrahigh vacuum use. They were used to control gas sample introduction to the residual gas analyzer (RGA) and for several other purposes, such as to control the calibrated leak. In addition to the advantages of a small internal volume and bakeability, these valves, unlike other all-metal valves, can be operated without releasing small amounts of gases into the vacuum system.

The large volume portion of the calibration system was sorbed out, pumped down, and baked out until the system pressure could be maintained at 10^{-10} Torr. Thereafter, this system was neither returned to atmospheric pressure nor exposed to the ambient atmosphere. Only the small volume portion was exposed so that calibrated leaks could be interchanged. Because dry nitrogen was used as backfill gas, only a brief bakeout was necessary to return the system pressure to the 10^{-10}-Torr range after a new calibrated leak was installed. A nude ionization gauge, visible in Fig. 4 but not shown in Fig. 3, was used to monitor the pressure during the initial pumpdown, but was not

Fig. 2. Dual Inlet Systems of the Mass Spectrometer

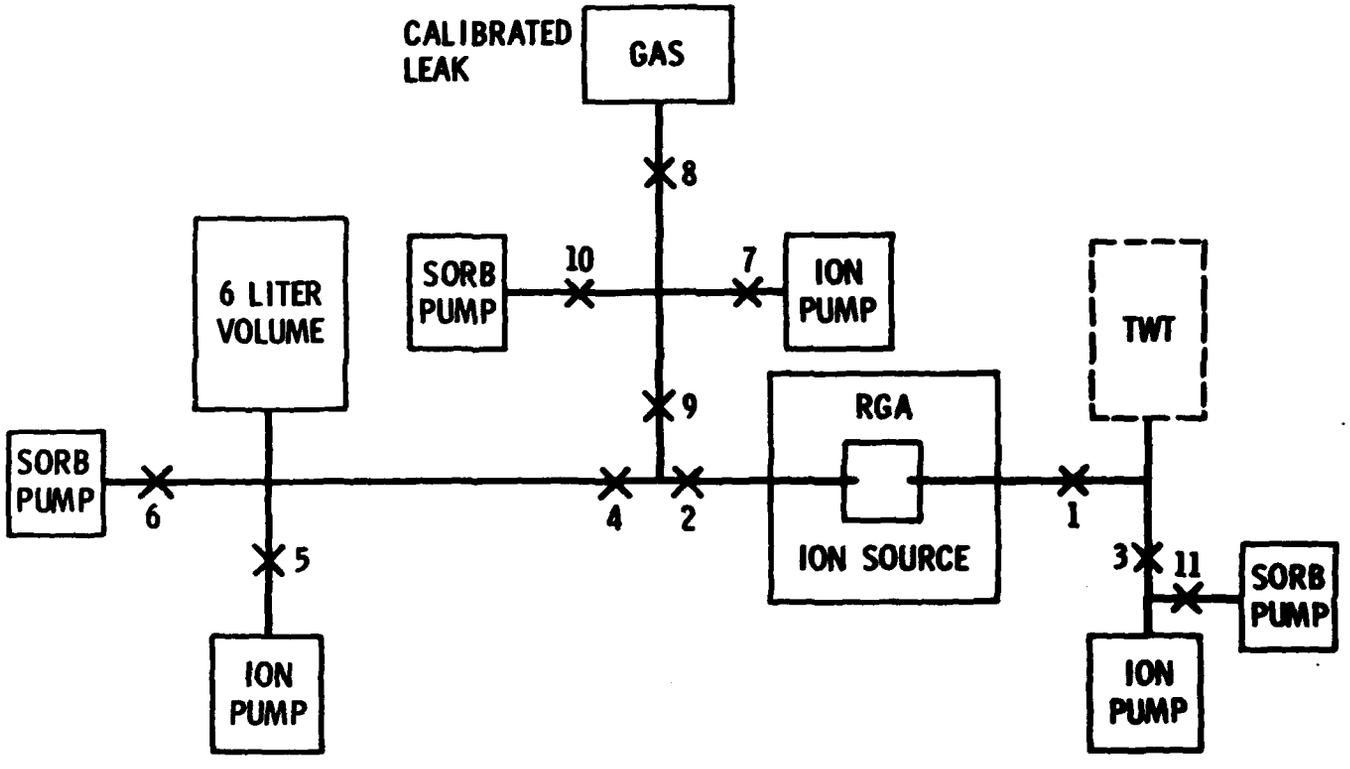

Fig. 3. Diagram of Calibration and RGA Sample Introduction Systems

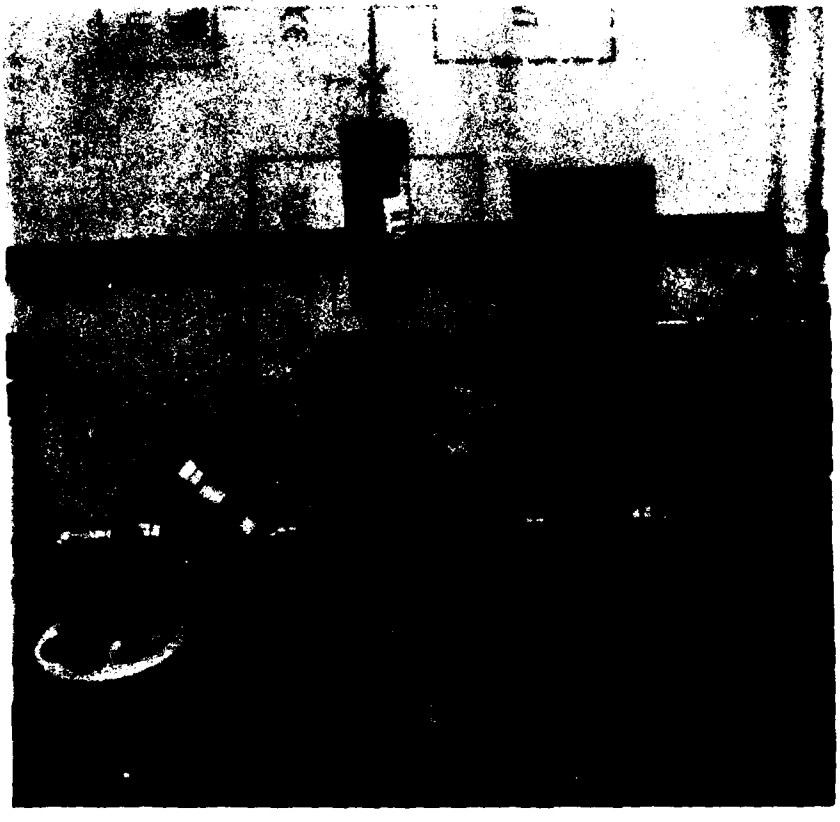

Fig. 4. Vacuum System for Calibration of the Mass Spectrometer

operated thereafter. The relative sizes of the large expansion volume, the small expansion volume, and the aliquot volume were in the approximate ratios of 1000::10::1 to facilitate the selection of a wide range of gas-sample sizes. These volumes were accurately determined in absolute units by dimensional measurement, and in relative units by pressure measurements or by gas analyses.

The reference standards to which all measurements of amounts of gas were related are calibrated gas leaks. Sixteen calibrated leaks of eight different gases were obtained from Teledyne-Hastings-Raydist and one leak was obtained from Leak Detection Systems, Inc. Leak rates, which ranged from 10^{-6} to 10^{-10} atm cm^3 sec^{-1}, were stated to be accurate to better than ±10% of the calibrated values.

III. METHOD OF CALIBRATION

The method of calibration of the mass spectrometer consisted of accumulating gas from a calibrated leak source in a large known volume for a precisely measured time interval, and then introducing a small measured aliquot of the large volume of gas into the spectrometer for analysis. The exact procedure followed is most easily described by referring to the calibration system portion of the diagram in Fig. 3.

The entire system, including the calibrated leak, was pumped down with the ion pumps; of course, valves #6 and #10, which connect with the sorption pumps, remained closed. Valve #8, which connects with the calibrated leak, was closed to start the accumulation of the gas sample; the timer was started simultaneously. About 1 min before elapse of the selected accumulation time, valves #2, #5, and #7 were closed to isolate the system from the ion pumps. If the aliquot sample was to be taken from the large volume, valve #4 remained open; if only the small volume was to be sampled, then it was closed. Thirty sec before the elapse of the time period, valve #8 was opened to allow the accumulated gas to expand into the selected volume. Valve #8 was closed to terminate the accumulation and the timer was simultaneously stopped. Valve #9 (and also valve #4, if it was not already closed) was closed to isolate the 4.7 cm^3 sample aliquot enclosed between valves #2, #4, and #9. Acquisition of background spectral data by the mass spectrometer was initiated about 30 sec before sample introduction and the ion gauge recorder was started at that time. Now valve #2 was rapidly opened and the gas sample was introduced to the analytical instrument. Although the sample was usually pumped out in less than 5 sec, 1 min was allowed before valve #2 was closed, and the acquisition of background spectral data was continued for another 30 sec. From the known leak rate, the measured accumulation time period, and the ratio of the aliquot volume to the sample expansion volume, the exact amount of the gas introduced for analysis was determined. This amount was related to measurements of the corresponding integrated area traced by the recorded ion gauge output and the integrated ion current of the RGA in digital counts corrected for the background response.

IV. RESULTS OF CALIBRATION MEASUREMENTS

For most of the analyses that will be described, the instrumental response has the same form that would be observed if a pulse of gas, such as the effluent from a gas chromatograph, had been introduced. An example of the pulse shape obtained with a relatively large sample of helium is given in Fig. 5. The recorded ionization gauge analog output is shown as a continuous curve, and the digital RGA data stored by the computer are plotted in bar graph format. By our standard, this was a large sample; only a few samples more than three times this size were introduced during the calibration studies. In spite of its size, the sample was completely pumped out in about 7 sec, as shown by the ionization gauge trace. Useful RGA data were also obtained for about 7 sec; therefore, with a scan rate of 2 scans per sec, about 15 data points were available for quantifying the analysis. Using the data shown in Fig. 5 and calibrations that will be given later, the amounts of helium determined by the ionization gauge and the RGA were 6.7×10^{-7} and 8.6×10^{-7} atm cm^3, respectively. These results bracket the value of 7.7×10^{-7} atm cm^3 obtained from the expansion and aliquot volumes, the sample accumulation time, and the 8×10^{-8} atm cm^3 sec^{-1} calibrated leak rate.

The helium sample from the previous illustration was larger than the amounts of residual gases expected to be found in traveling wave tubes, although subsequent results of analyses showed that several tubes contained even larger amounts of gases. As a contrast to the last example, Fig. 6 presents the digital RGA data in the format of the RGA plotter to demonstrate that a helium sample as small as 7.4×10^{-12} atm cm^3 can be successfully transported to the RGA and analyzed. The 3×10^{-10} atm cm^3 sec^{-1} calibrated leak was used to obtain this helium sample during a 30-sec accumulation period. Although this does not represent the detection limit of the RGA, it was not feasible to introduce a smaller known amount of gas to the RGA for analysis. For the analysis shown in Fig. 6, an electron multiplier voltage higher than the usual 1700 V was used for the analyses. The scan-to-scan variation in the background signal was amplified as a result of the higher multiplier voltage;

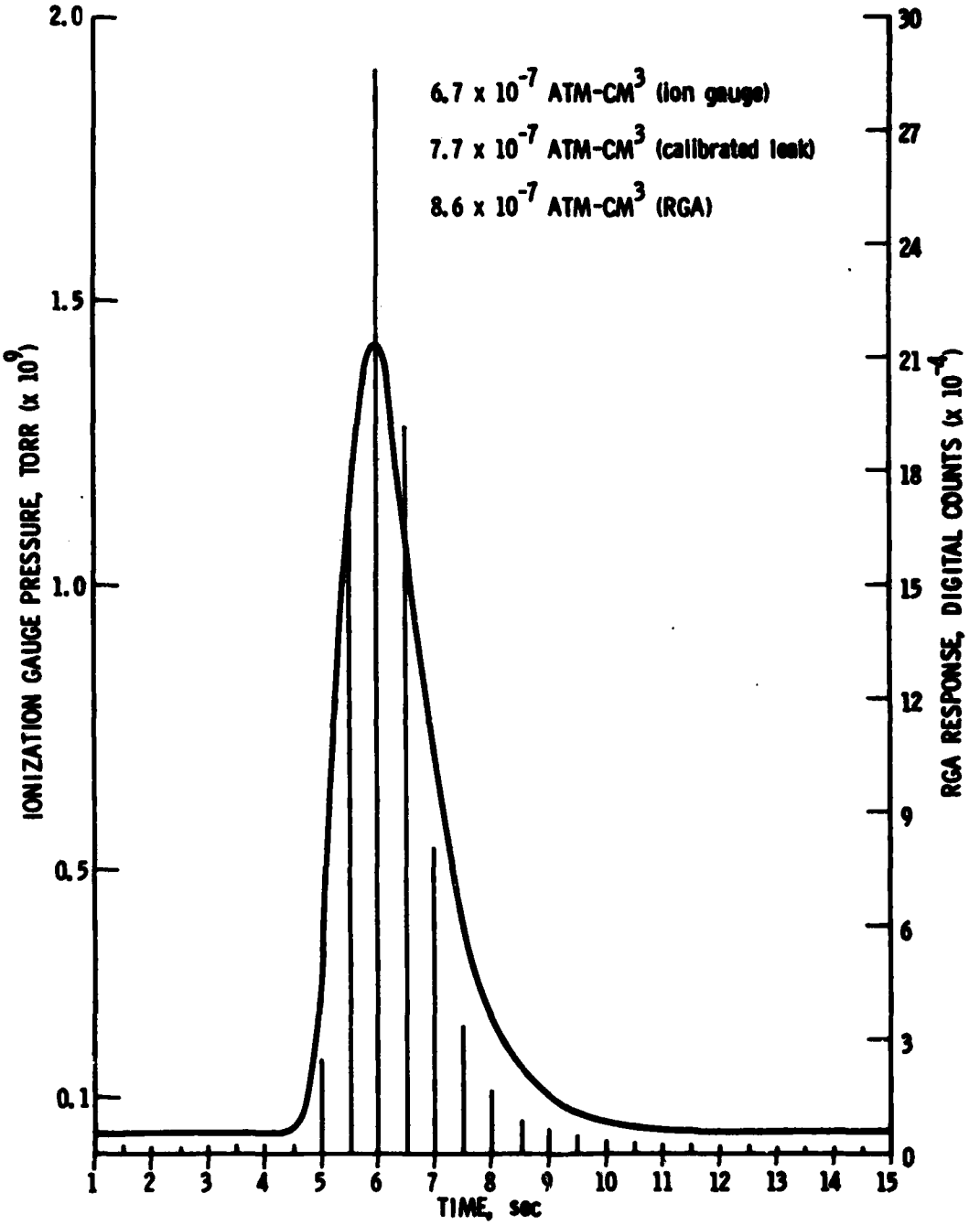

Fig. 5. Pulse Shape of Relatively Large Helium Sample Analyzed by RGA and Ion Gauge

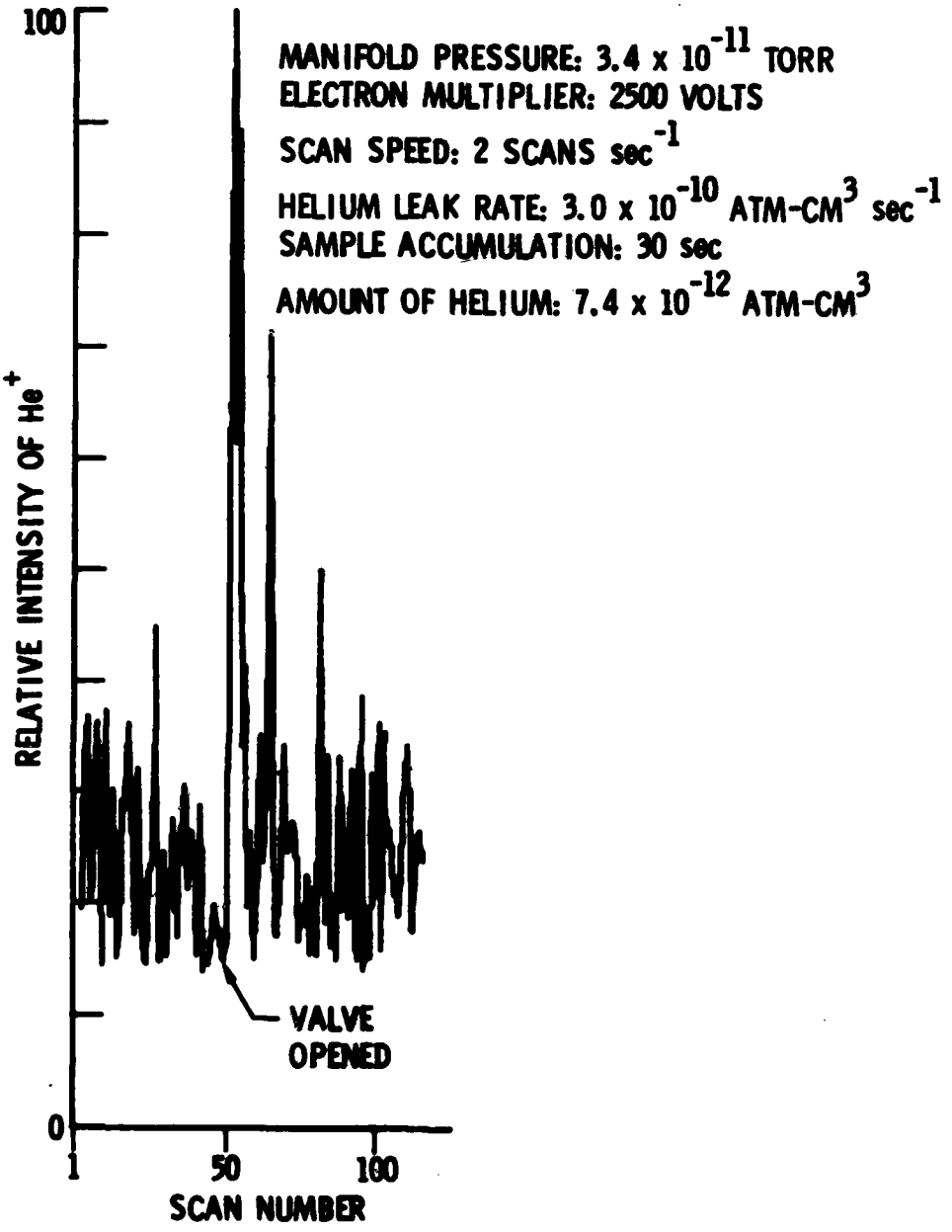

Fig. 6. RGA Analysis of Ultramicro Sample of Helium

nevertheless, when the valve was opened at scan no. 50, the appearance of the helium pulse was unmistakable. It is of interest to note that 7.4×10^{-12} atm cm^3 of gas corresponds to fewer than 200 million molecules. We consider it remarkable that this small an amount of gas exhibits transport and ionization cross-section characteristics similar to those shown by amounts of gas that are as much as eight decades larger.

The linear response of the RGA to gas samples that ranged in size over four decades is demonstrated for five of the gases tested in Fig. 7 through 11. The data for hydrogen shown in Fig. 10 are incomplete because the capillary of a 10^{-9} atm cm^3 sec^{-1} calibrated leak became clogged.

Reproducibility of the RGA measurements was good, as is demonstrated in Table 1. The standard deviations from the average values are given only for the analyses of very small samples. For larger samples, the reproducibility was better. The large background correction for residual hydrogen in the RGA and the short accumulation time made necessary by the higher leak rate from the 10^{-8} atm cm^3 sec^{-1} calibrated leak cause the RGA measurements of small hydrogen samples to be less reproducible.

Several calibrated leaks with leak rates differing by at least one decade were available for each of the gases except argon and carbon monoxide. For each of the other gases, measurements using the different leaks are distinguished in the plots of the results. Consistency of the results obtained with leak rates that spanned as much as three decades is indirect evidence of the accuracy of the calibrations. In Fig. 7, the results of measurements are given for three helium-calibrated leaks with leak rates of 3×10^{-10}, 3×10^{-9}, and 8×10^{-8} atm cm^3 sec^{-1}. Agreement of the results is good, even though the smallest leak was obtained from a different manufacturer. Even better agreement is exhibited by the results shown in Fig. 9 for two nitrogen leaks with leak rates of 3×10^{-9} and 2×10^{-7} atm cm^3 sec^{-1}. Consistent results were obtained with the two hydrogen leaks with leak rates of 3×10^{-8} and 6×10^{-7} atm cm^3 sec^{-1}. An obstruction in the extremely fine-bore capillary required for a 10^{-9} atm cm^3 sec^{-1} hydrogen leak prevented our obtaining

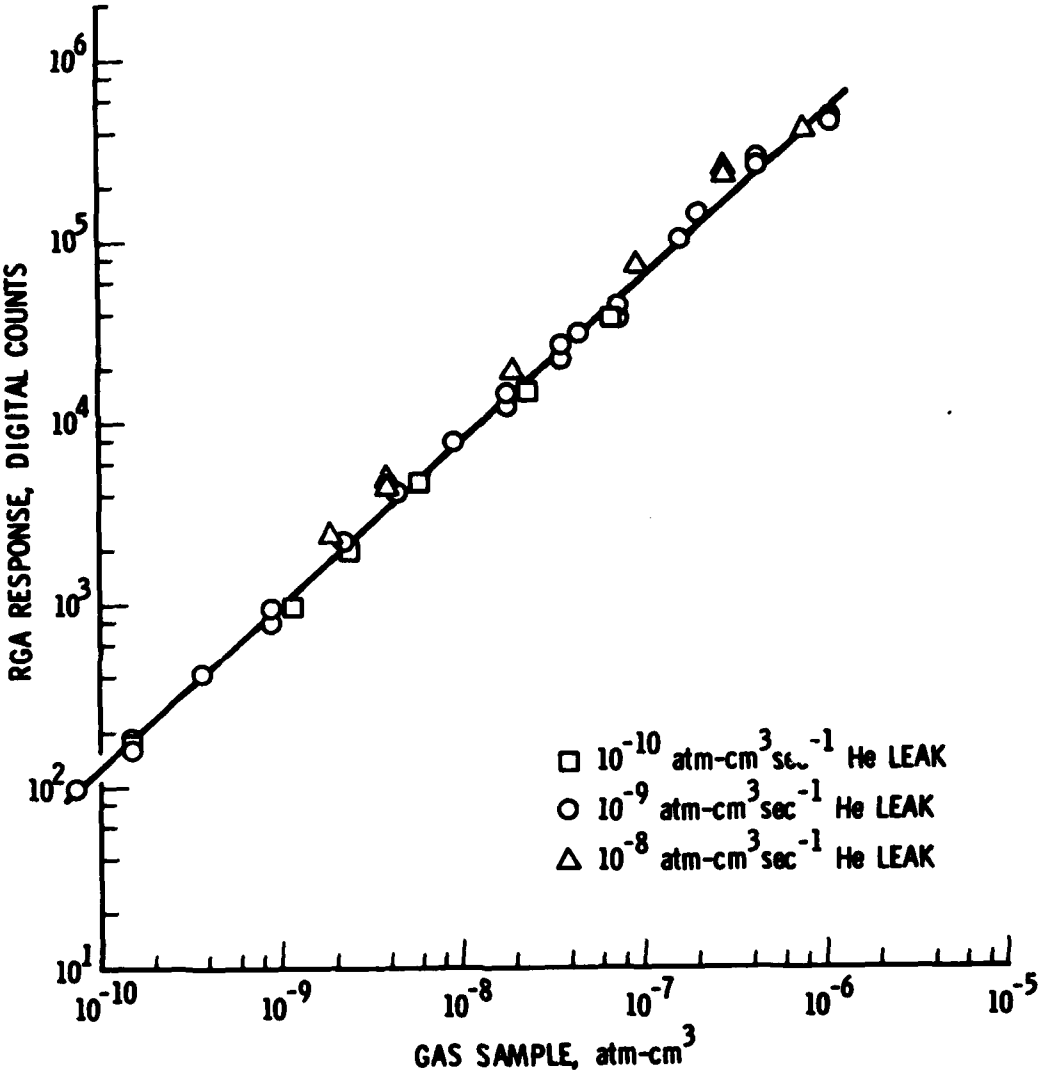

Fig. 7. RGA Calibration for Helium

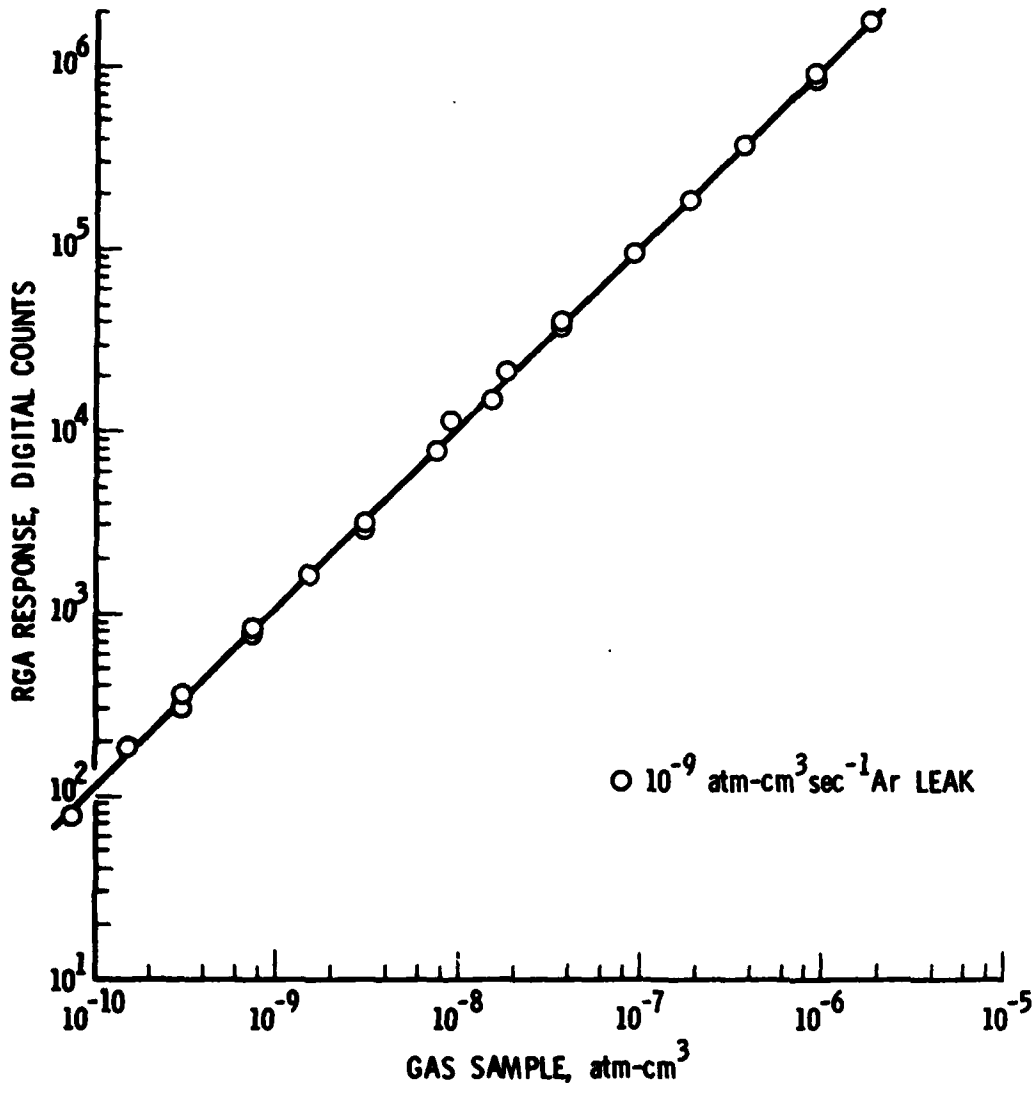

Fig. 8. RGA Calibration for Argon

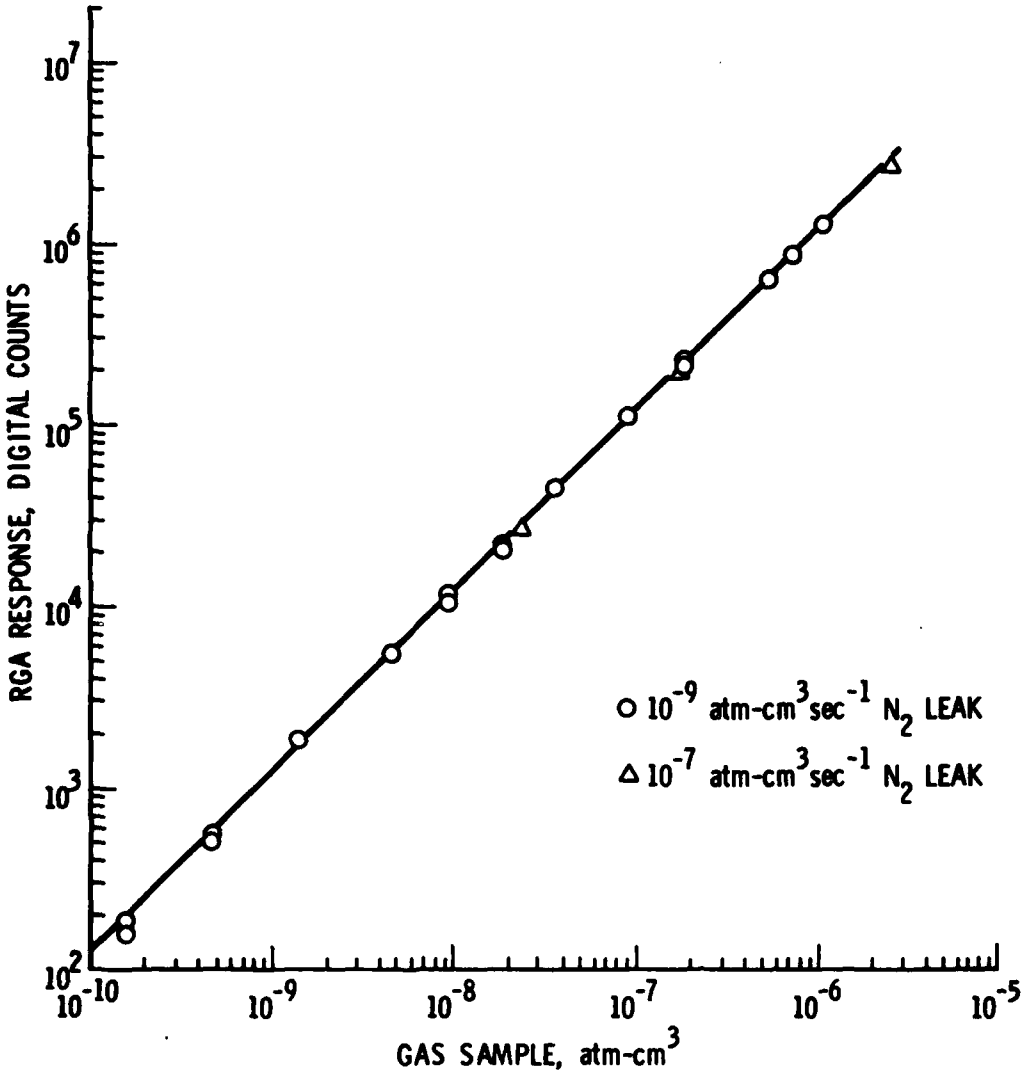

Fig. 9. RGA Calibration for Nitrogen

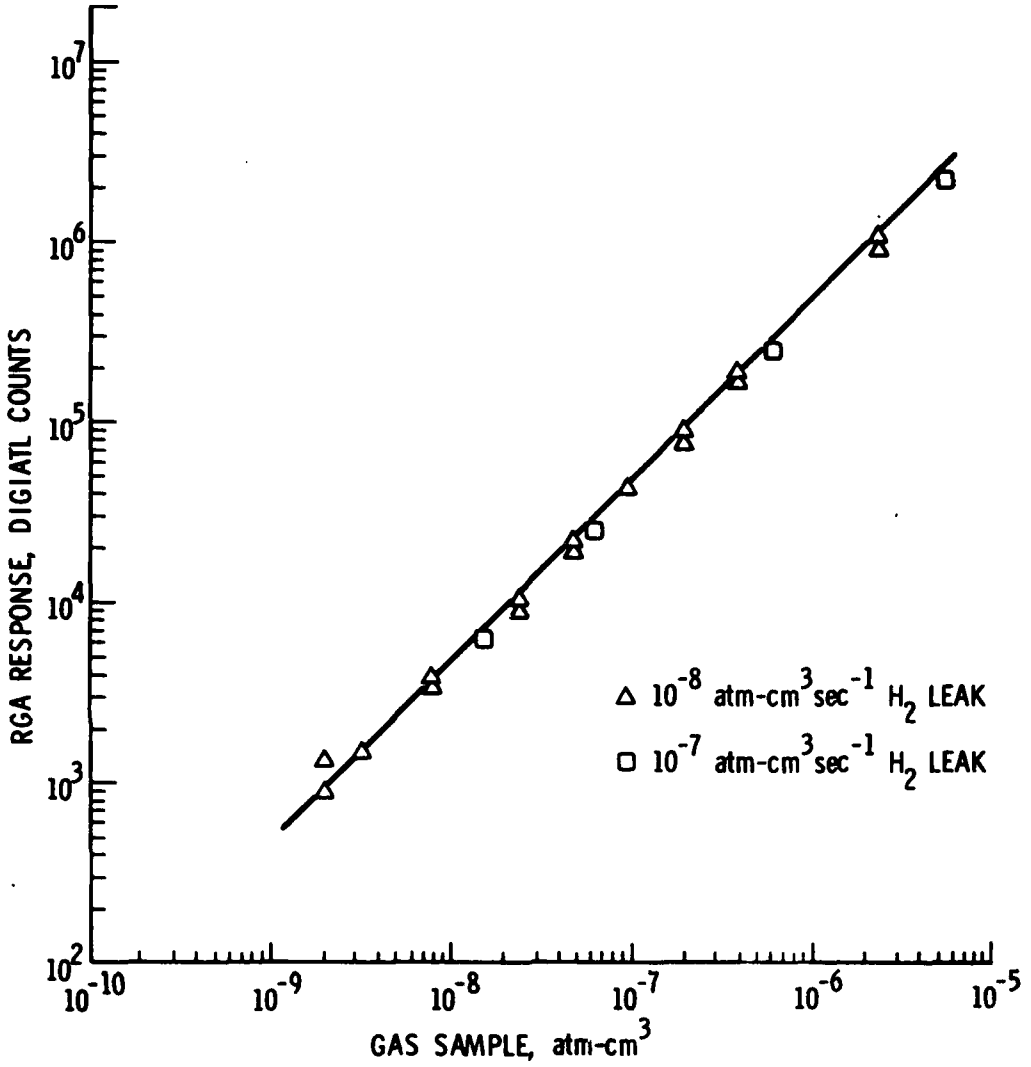

Fig. 10. RGA Calibration for Hydrogen

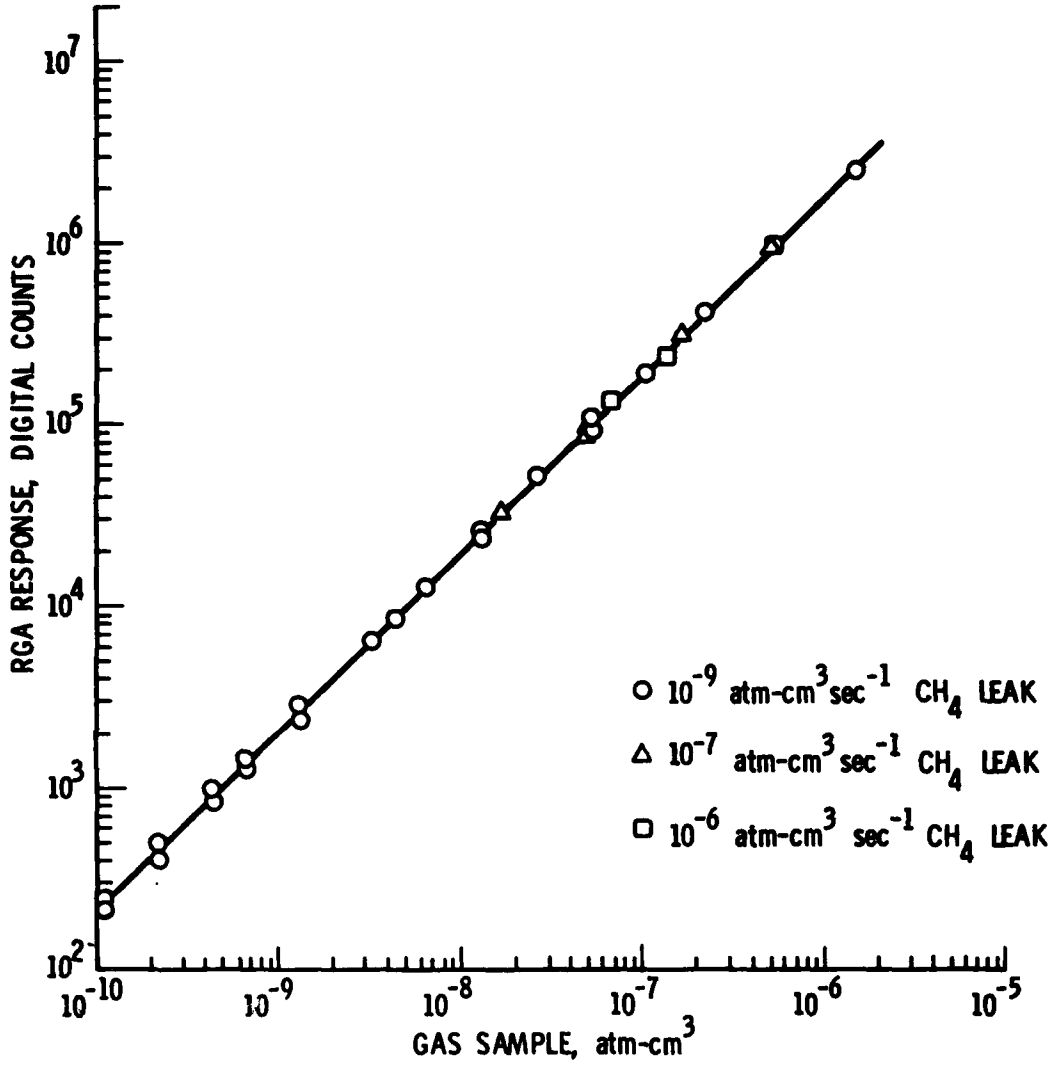

Fig. 11. RGA Calibration for Methane

Table 1. Reproducibility of Analyses of Small Amounts of Gases

Gas	No. of Analyses	Average Amount, atm cm^3	Standard Deviation
Helium	4	9×10^{-10}	9%
Argon	5	2×10^{-10}	8%
Nitrogen	6	1×10^{-9}	10%
Hydrogen	4	2×10^{-9}	17%
Methane	5	4×10^{-10}	5%

data from a third hydrogen-calibrated leak. The most striking agreement of the results is shown in Fig. 11 for the three methane leaks with leak rates of 4×10^{-9}, 3×10^{-7}, and 2×10^{-6} atm cm^3 sec^{-1}. The three methane leaks were constructed and calibrated by the supplier over a period of more than four years. It is almost inconceivable that there could be gross inaccuracies of the calibrations in view of the remarkable consistency of the results of our measurements.

Figures 12 through 14 are plots of the results of measurements with three gases that showed evidence of interaction with the walls of the metal vacuum system. For both carbon monoxide and carbon dioxide, the results of the calibration measurements depended on whether the larger or the smaller expansion volume was used. The results, which have been plotted in Figs. 12 and 13 to distinguish the volumes used, indicate that greater losses of each gas occurred when the volume with the larger surface area was used. There was also more scatter of the data points when the larger volume was used, indicating greater variation among measurements, which probably resulted from slight differences in sample exposure times. An apparent inverse dependence of the results on the sample accumulation time is indicated in Fig. 13 by the slightly larger RGA response values obtained with a 25-fold-larger leak rate of carbon dioxide. The results show that both carbon monoxide and carbon dioxide can be quantitatively analyzed in amounts as small as 10^{-9} atm cm^3 if the samples do not encounter large wall surface areas during transport to the RGA.

For oxygen, the results shown in Fig. 14 are not easily interpreted. It was apparent that oxygen interacted rather strongly with surfaces in the vacuum system. However, samples as small as 10^{-8} atm cm^3 could be analyzed if the smaller expansion volume was used. When relatively large accumulated oxygen samples were expanded into the larger volume, subsequent analyses showed that complete retention of the gas on the walls had occurred. In fact, the magnitude of the RGA response for oxygen was comparable to that for the other gases, but it increased proportionately as the sample size was decreased. This may have been the result of shorter sample accumulation times if the rate of interaction of the gas with the walls is sufficiently slow.

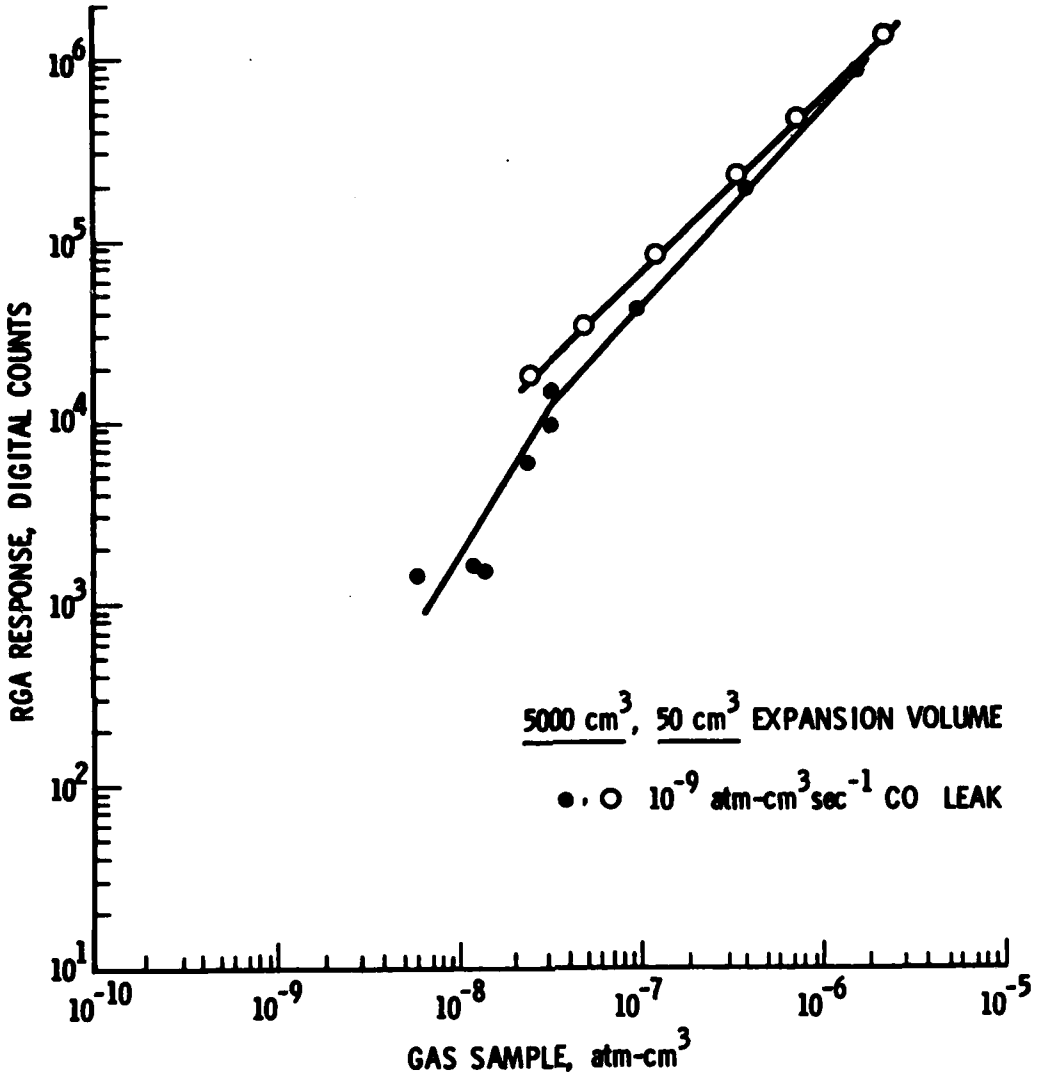

Fig. 12. RGA Calibration for Carbon Monoxide

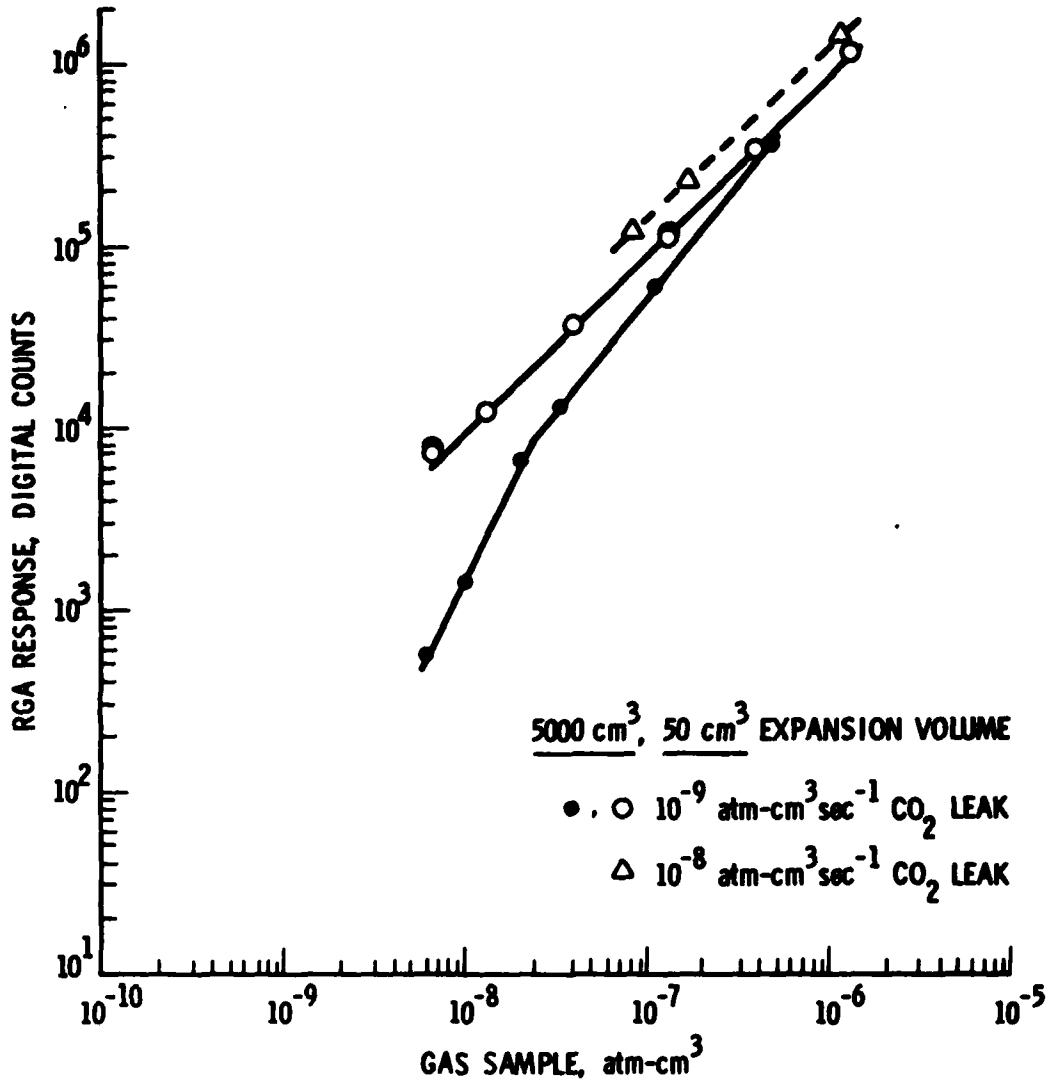

Fig. 13. RGA Calibration for Carbon Dioxide

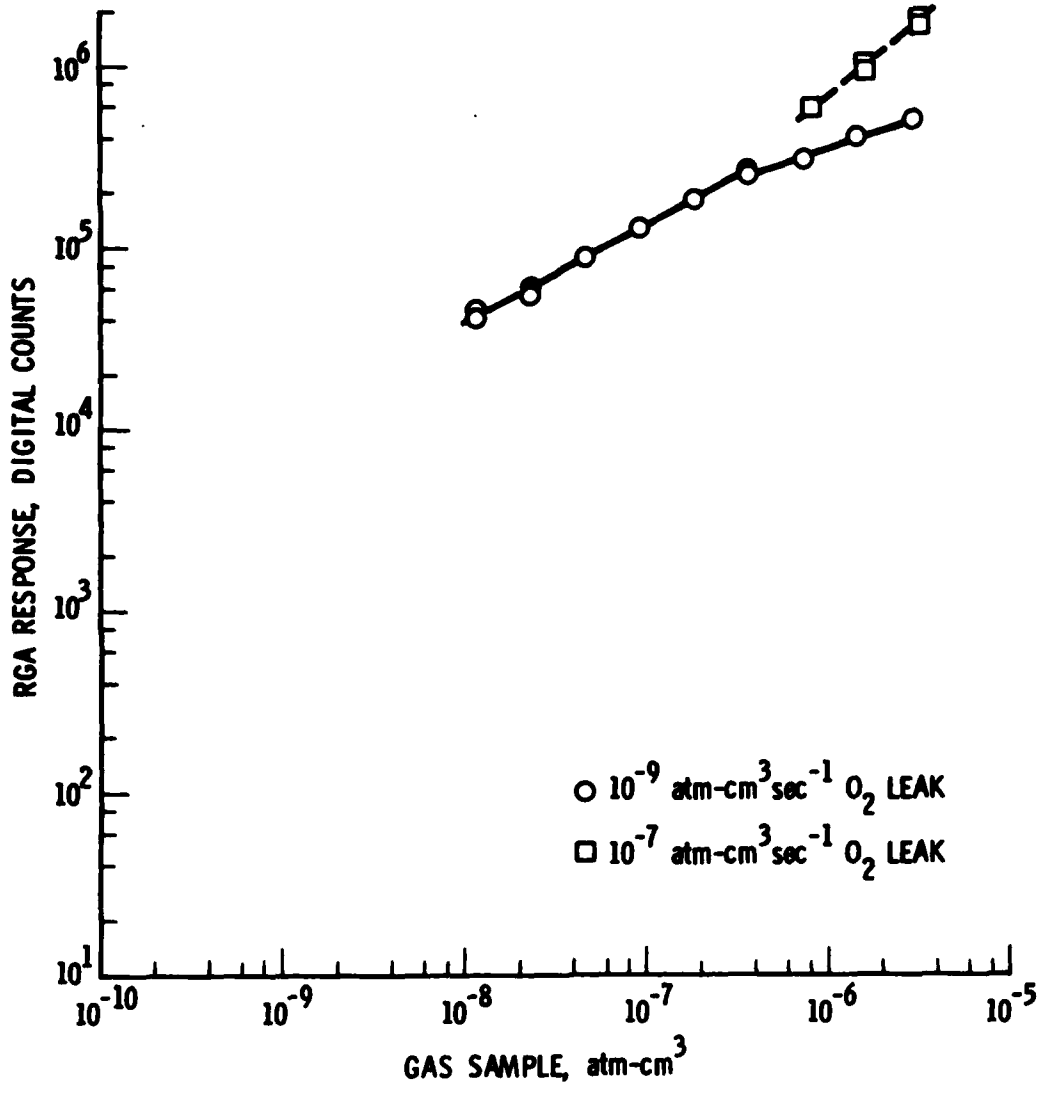

Fig. 14. RGA Calibration for Oxygen

Additional evidence for this hypothesis is shown in Fig. 14 by the significantly higher RGA responses obtained from oxygen samples that were accumulated much more rapidly from a calibrated leak with a 70-fold-higher leak rate. More data are needed for a complete understanding of the behavior of small amounts of oxygen in metal vacuum systems. However, oxygen has not been detected in the analyses of the residual gases from any of the devices that have been received. Therefore, it has not been necessary to pursue the investigation of its behavior. The data of Figs. 7 through 13 plotted on full logarithmic grids have been fit by least squares to straight lines. An alternate representation of the equation for the straight line is

$$\text{RGA response (digital counts)} = b \{ \text{gas sample (atm cm}^3 \times 10^{10}) \}^m \qquad (1)$$

The b and m parameters of equation (1) obtained from the least squares fit of the data for seven of the gases are tabulated in Table 2. For CO and CO_2, the data obtained with the smaller expansion volume were used.

It is evident that the m parameter indicates the order of proportionality of the empirical calibration expression (1), and the b parameter indicates the relative response of the RGA for a particular gas. For five of the gases, the order of proportionality closely approaches unity. Over a four-decade range in sample size, the deviations from a direct proportionality would amount to 2, 10, 14, and 15% of N_2, Ar, H_2 and CH_4, or CO_2, respectively. Although the slight deviation of the m parameter from unity for CO may be attributed to the interaction with the wall surfaces, the low value for helium is not easily explained. Two possibilities come to mind, but neither has additional supporting evidence. One possibility is that helium is ion pumped more efficiently at higher pressures, unlike the other gases, or alternatively, that it permeates into the glass wall of the calibrated leak, or into voids that are not discharged rapidly enough for the gas to be included in the pulse. Neither explanation is entirely satisfactory, because the shape of the helium pulse as a function of the size of the gas sample is not different from the pulse shapes of the other gases.

Table 2. MGA Calibration Data Parameters

Gas	m	b
Helium	0.904	81
Argon	0.989	116
Nitrogen	0.998	121
Hydrogen	0.984	54
Methane	0.982	210
Carbon Monoxide	0.964	90
Carbon Dioxide	0.982	101

An examination of the b parameter values in Table 2 shows that there is less than a four-fold range of RGA responses for the seven gases. The gases can be arranged in three groups, with H_2 showing one-half the sensitivity, and CH_4 twice the sensitivity, of N_2, Ar, He, CO, and CO_2. The lower sensitivity of helium and hydrogen is expected, but that of carbon monoxide is not. The demonstrated tendency of carbon monoxide to interact with wall surfaces is a probable cause. Although the instrument was adjusted to enhance the response to the low atomic mass ions, the high sensitivity of methane has not been satisfactorily explained.

Because the b parameters of Table 2 derive from extrapolations of the curves in Figs. 7 through 13 to the ordinate corresponding to 1×10^{-10} atm cm^3, they are rather inexact. In fact, it was necessary to use logarithmic data for the least squares fitting in order to obtain reasonable values of the b parameter. To compare the RGA responses for the different gases, it is preferable to analyze a common sample size of each gas. This can be done by accumulating and analyzing the same amount of each gas, or by transporting the effluent of the respective calibrated leaks directly into the RGA for analysis. In the latter case, corrections must be made for the differences in the leak rates of the calibrated leaks. A common leak rate of 1×10^{-10} atm cm^3 sec^{-1} was selected to make the data numerically equivalent to the b parameters; the results for accumulated samples were normalized to a sample size of 1×10^{-10} atm cm^3 for the same reason.

An illustration of the two analyses is given in Fig. 15. The effluent from the leak was analyzed after the analysis of a 6-min accumulation of argon from the 3.0×10^{-9} atm cm^3 sec^{-1} calibrated leak. The leak was not closed off at the conclusion of the sample accumulation, so the effluent from the leak continued to enter the RGA after the accumulated sample had been pumped away.

The results of these two alternate methods of comparison are shown in Table 3. These data are not markedly different from the corresponding values of the b parameter shown in Table 2. The results for oxygen were obtained from a few measurements that appeared to be consistent and reproducible.

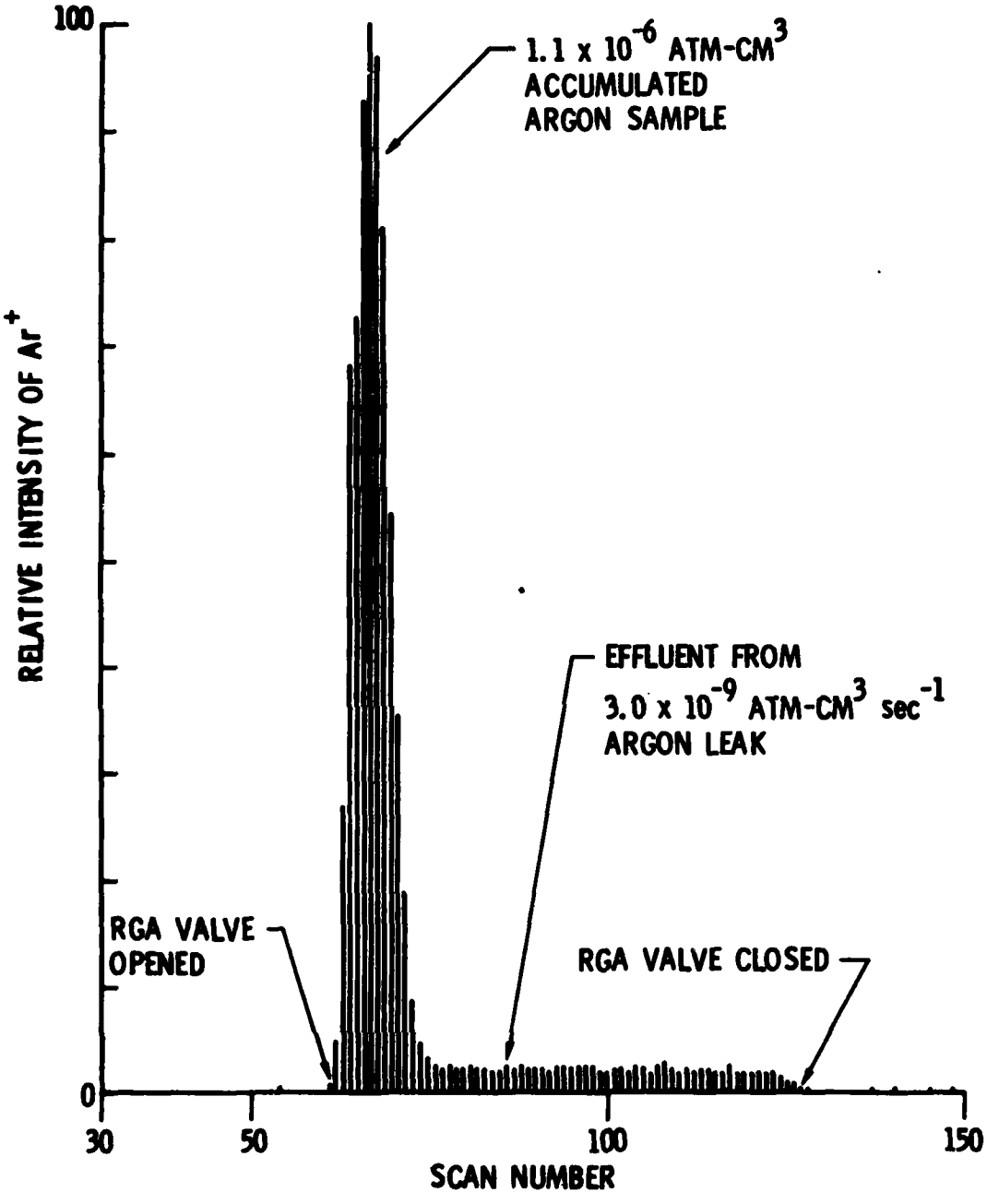

Fig. 15. RGA Analysis of Relatively Large Accumulation and Effluent of Argon-Calibrated Leak

Table 3. RGA Responses for Different Gases Using Both Pulsed and Continuous Sample Introduction

Gas	Average of Analyses of Accumulated Samples, Digital Counts $\times 10^{-10}$/atm cm^3	Analysis of Effluent of Calibrated Leaks, Digital Counts $\times 10^{-10}$/atm cm^3 sec^{-1}
Helium	49	48
Argon	80	78
Nitrogen	111	113
Hydrogen	55	57
Methane	211	209
Carbon Monoxide	68	60
Carbon Dioxide	93	101
Oxygen	37	41

There is excellent agreement between the two sets of data, one obtained by analysis of a steady flux of sample, the other from analysis of a pulse of accumulated sample. This agreement supports the validity of the dynamic method of analysis.

Additional evidence to support the RGA response data was obtained from the results of the ionization gauge calibrations. It was discovered that the nude ionization gauge, located in the manifold of the RGA directly above the closed ion source chamber, functioned as a sensitive detector of the total amount of gas introduced to the RGA for analysis. The shape of the curve produced by the recorded output of the ionization gauge controller is shown in Fig. 5. A planimeter was used to measure the area bounded by the curve generated when a known gas sample was introduced. A linear relationship was found between these areas, which were corrected for any recorder scaling factor, and the amount of gas introduced to the RGA. Examples of this relationship that span almost four decades are shown for argon, nitrogen, and helium in Fig. 16. The orders of proportionality from the slopes of the curves of Fig. 16, determined by least squares, are 0.98 for argon, 1.02 for nitrogen, and 0.94 for helium. The results for helium were obtained with the use of the all-metal 10^{-10} atm cm^3 sec^{-1} calibrated leak.

We found it extraordinary that the ionization gauge of the RGA was sufficiently sensitive to detect amounts of gas as small as 10^{-10} atm cm^3. Of course, the ionization gauge cannot distinguish the gases, although the response of the ionization gauge is not constant for all the gases, as shown by the data of Table 4. The two sets of ionization gauge response data were obtained from measurements that were entirely analogous to the two alternative measurements of RGA response. For those measurements made with accumulated gas samples, the transitory ionization gauge readings have been integrated over the pulse period, as previously described, and then normalized to a common sample size of 3×10^{-10} atm cm^3. The sample size was arbitrarily selected so that there would be numerical equivalence of the results for both sets of data. The second set of data was obtained from the ionization gauge readings that were invariant with time while the effluents from the calibrated leaks were directed into the RGA. For these measurements, the increases in

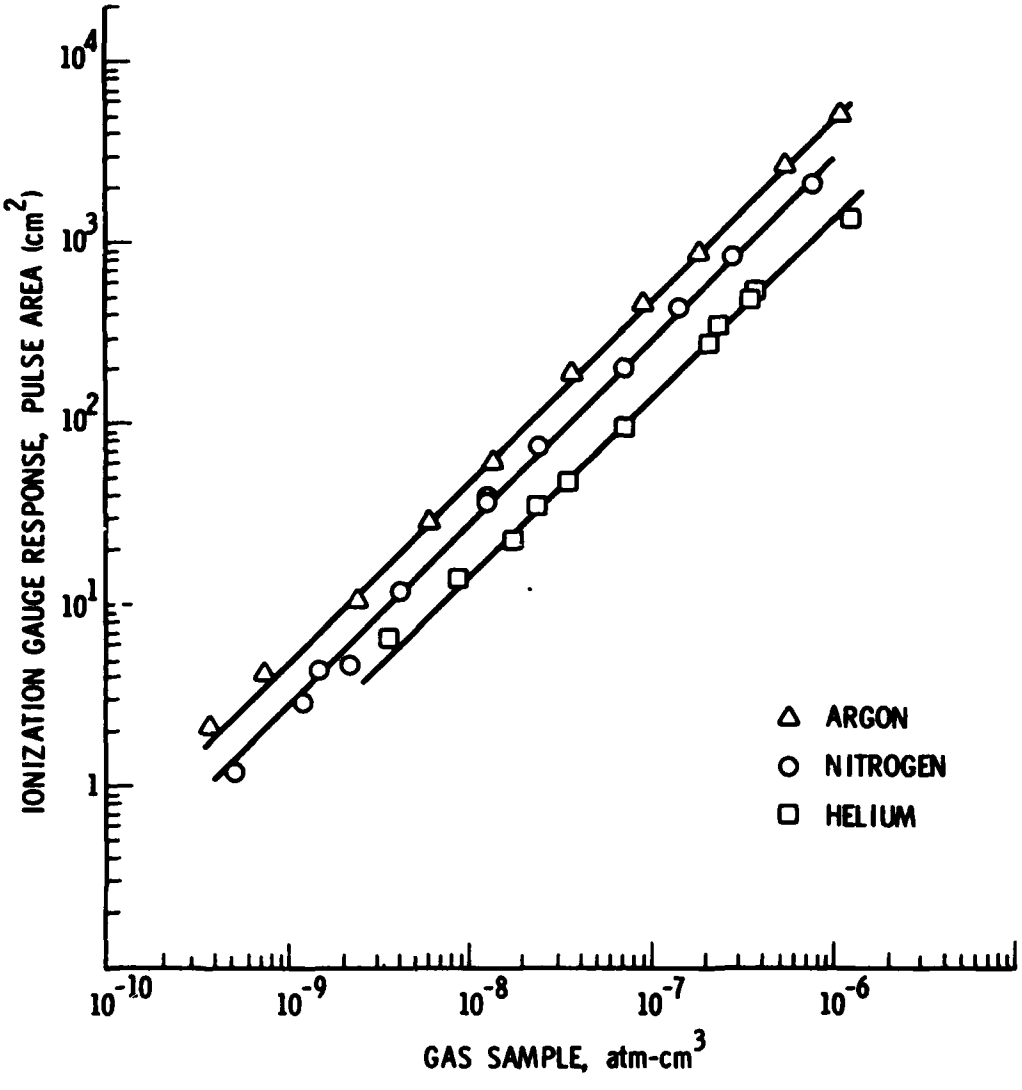

Fig. 16. Ionization Gauge Calibration with Several Gases

Table 4. Ionization Gauge Responses for Different Gases Using Both Pulsed and Continuous Sample Introductions

Gas	Average of Accumulated Samples (Integrated Pulse Area), $cm^2 \times 3 \times 10^{-10}$/atm cm^3	Effluent of Calibrated Leak, Torr $\times 10^2$/ atm cm^3 sec^{-1}
Helium	0.46	0.45
Argon	1.49	1.49
Nitrogen	0.98	1.03
Hydrogen	0.14	0.13
Methane	1.31	1.27
Carbon Monoxide	0.43	0.47
Carbon Dioxide	0.86	1.10
Oxygen	0.35	0.40

the pressure above the background level have been normalized to a common leak rate of 10^{-2} atm cm^3 sec^{-1}.

The numerical agreement between the two sets of data of Table 4 shows that the relative results are consistent for both methods of sample introduction. This is further testimony for the validity of the dynamic method of analysis. Of the data shown in Table 4, only the relative results for hydrogen, oxygen, and carbon monoxide are not in approximate agreement with published relative values obtained from measurements under static conditions at much higher pressures (Refs. 3, 4). Our lower results for these gases can be attributed to interactions with the heated filament of the RGA ion source chamber, through which the gas must pass before reaching the ionization gauge.

After bakeout of the RGA vacuum system and prolonged pumping over a period of many months, the pressure indicated by the ionization gauge with a RGA source emission current of 0.5 mA gradually decreased to a steady level of about 3×10^{-11} Torr. Although this RGA operating pressure was not reduced further by operation of the titanium sublimator, it did not appear that this was the x-ray limit of the ionization gauge. It has already been shown that at this limiting pressure the gauge was still responding in a linear manner to very small amounts of gases. Furthermore, the total ion current of the RGA, produced by background gas in the vacuum system, had also reached a stable minimum value. Apparently, the system had established a steady-state between outgassing rates and ion pumping rates which would be maintained indefinitely unless there was additional baking, perhaps at higher temperatures. Since this operating pressure was low enough theoretically for the analyses that were planned, and because subsequent experience demonstrated that it was adequate, no attempt was made to reduce it still further.

A typical spectrum of the residual background gas in the mass spectrometer is shown in Fig. 17. It is apparent that hydrogen is the predominant species. The peaks corresponding to O^+, F^+, and Cl^+ are caused by electron bombardment of source materials and do not correlate with the gas composition (Refs. 5, 6). Furthermore, if one takes into account the slightly lower sensitivity of the RGA to hydrogen, it can be concluded that approximately 98%

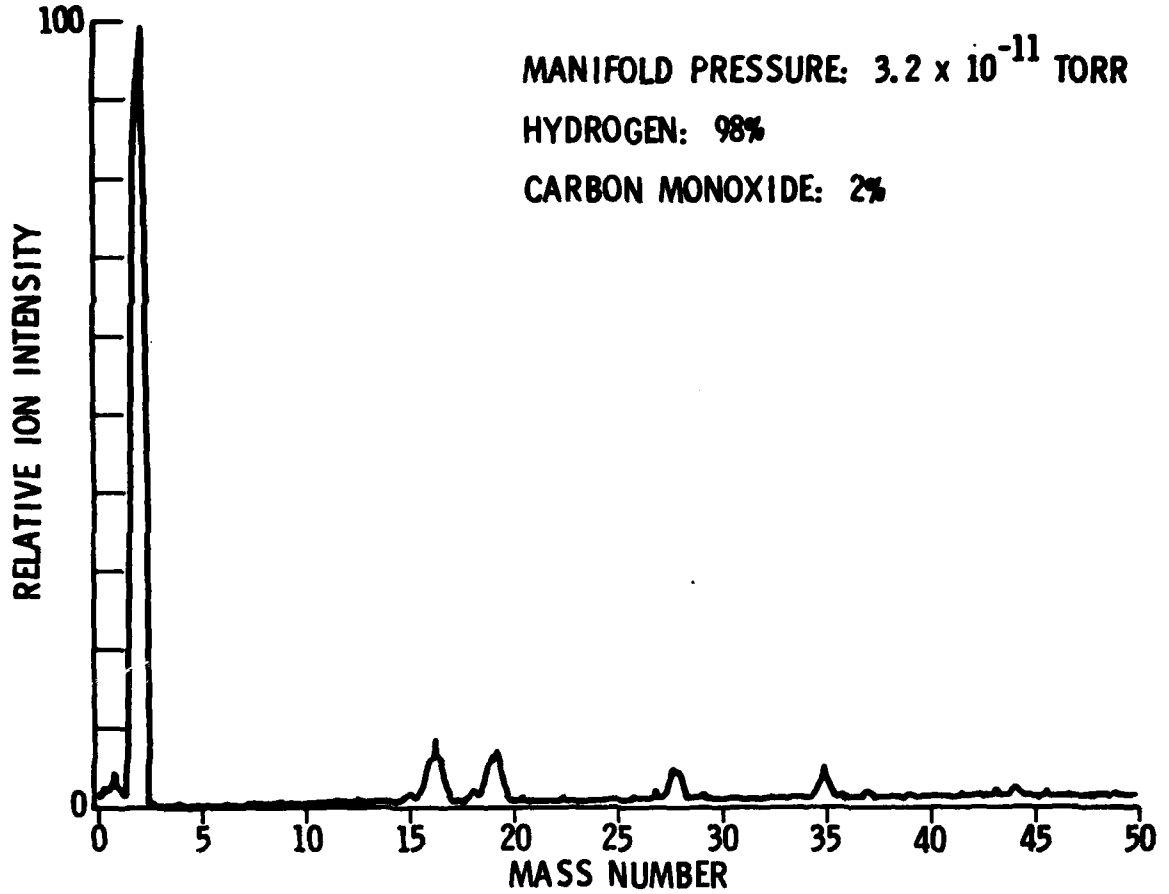

Fig. 17. RGA Background Spectrum

of the background gas in the RGA is hydrogen. This observation is in agreement with the results of our residual gas analyses obtained with other well-baked, stainless-steel-walled vacuum chambers.

Most of the results of calibration measurements were obtained with the RGA operating under the conditions just described. After more than 2.5 years of operation, the original source had to be replaced and the system pressure is again slowly decreasing toward its previous minimum level. At present, it is about a factor of two higher than its previous lowest value. A repetition of the calibration measurements showed that in most cases the results obtained after replacing the source were lower by only 10% than corresponding values obtained previously. There were certain notable exceptions, however. For the gases that had previously shown a tendency to interact with the walls, i.e., carbon monoxide, carbon dioxide, and oxygen, the results of the most recent calibrations correspond to increases of as much as a factor of two in the responses of both the RGA and the ionization gauge. The cause of this change is not known at present.

The cause of another difference between the results of measurements before and after replacement of the ion source is understood. A calibrated leak of each of 7 gases in turn was installed in the location labeled TWT in Fig. 2 to compare the RGA response with the value obtained when the same leak was in the original location on the calibration system. This was done to compare the relative RGA sensitivities for gas sample introductions to the source through the two alternative ports. While the original source was still operational, the sensitivities measured through the TWT inlet port were lower by an average of 15% (with a standard deviation of 3%) for the 7 gases that were tested. When the manifold was opened to replace the source, the cause of this difference was discovered, but unfortunately was not corrected.

Since the source chamber is not at the same electrical potential as the wall of the vacuum system, the tubulation from the inlet valve to the source is completed by means of a short length of glass tubing. It was found that the TWT inlet tubulation was slightly misaligned. This caused a small fraction of the gas sample to bypass the source. Apparently, when this tubulation

was reassembled after replacement of the source, the condition was exacerbated. At present, the RGA sensitivity at the TWT source inlet port is about one-half that at the opposite port. However, very nearly the same response of the ionization gauge is observed with gas introduction from either port. Therefore, although the RGA ion source sees only a portion of the gas sample introduced through the TWT inlet, the ion gauge responds to the entire sample.

V. APPLICATIONS OF ANALYTICAL METHOD

It was not the purpose of this report to include detailed descriptions of the analyses for residual gases in microwave amplifier tubes. However, it is appropriate to conclude this report with a brief illustration of the application of our dynamic analytical method. Residual gas analyses have been conducted for 25 devices with the results shown in Table 5. Although the individual devices have been purposely left unidentified, they can be grouped according to the composition of the residual gases that were found. One group contained argon predominantly. Another group contained either methane or hydrogen, or a combination of both gases. A third group contained principally helium and methane. The total amounts of gas found by analysis ranged from more than 10^{-5} atm cm^3 to less than 10^{-9} atm cm^3. These amounts were corroborated in many cases by the results of an independent measurement made before the gas analysis, as shown in Table 5.

A method for determining the gas pressure in a device containing an electron emitter and suitably spaced electrodes has been reported (Ref. 7). The device is operated in much the same way as an ionization gauge. The gas pressure is determined from measured electron emission currents, ion currents, and a proportionality constant obtained by calibration. With this method it was possible to estimate the amount of gas in the device before the analysis was attempted, and this was of considerable assistance. For example, it was shown that most of the gas had been ion-implanted in surfaces of the traveling-wave tubes, and was only released by heating during operations that were preparatory to the analyses.

The results of analysis of the residual gas in two traveling-wave tubes have been selected to illustrate the direct applicability of the calibration measurements. Each of the traveling-wave tubes was welded to a puncture assembly that was then attached to the vacuum system (Fig. 3), evacuated, and baked to achieve ultrahigh vacuum conditions. To obtain ingress, the wall

Table 5. Results of Gas Analyses of 25 Traveling-Wave Tubes and Diodes

Amount of Gas, $\times 10^7$ atm cm^3		Gas Composition, %				
Calculated from Ion Currents	RGA Analysis	H_2	He	CH_4	CO/N_2	Ar
0.14	0.17	-	-	-	-	100
0.075	0.065	-	14	-	-	86
0.046	0.066	-	-	-	48	52
0.50	2.7	-	-	97	-	3
1.5	1.8	-	-	-	-	100
4.8	2.1	-	18	-	-	82
30	13	-	-	-	10	90
24	13	1	-	1	-	98
37	40	1	-	-	-	99
2.6	0.54	33	-	3	14	50
-	38	1	-	1	-	98
37	13	73	-	21	4	2
0.066	< 0.01	-	-	-	-	-
2.3	107	13	-	87	-	-
23	7.4	93	-	1	3	3
45	250	72	-	20	8	-
32	270	65	-	27	8	-
11	27	3	-	79	9	8
0.68	0.69	-	-	93	-	7
0.17	0.62	-	-	98	-	2
0.12	0.021	-	-	-	-	100
-	13	2	36	61	-	1
-	17	6	47	40	1	6
-	490	-	1	99	-	-
-	0.31	-	72	-	-	28

of the TWT was punctured with a pin attached to a linear motion vacuum feedthrough. The residual gas, now distributed in both the TWT and the puncture assembly, was introduced to the RGA through valve no. 1 (Fig. 3).

In the first example the residual gas in a 40-W TWT was analyzed, with the results shown in Figs. 18, 19, and 20. When the valve was opened at scan no. 138, the gas was transported through the ion source chamber in the form of a pulse, as shown in Figs. 18 and 20, similar to those pulses observed in the calibration measurements. A slight tailing of the pulse is the only evidence of the effect of transporting the gas remaining in the TWT through the pinhole. The composition of the gas can be obtained from the mass spectrum corresponding to any scan between 140 and 180. The mass spectrum shown in Fig. 19 is from scan no. 156, after subtraction of the background. The only significant ions observed were Ar^{+} (mass 40) and Ar^{++} (mass 20). However, there is a more accurate method of determining the gas composition that averages the analytical data for all the relevant scans. The pulse shown in Fig. 18 was produced from the summation of the intensities of all ions generated in the RGA for each mass spectral scan. In addition to the composite pulse from all ions, the computer has stored the intensity of each ion fragment for each of the mass spectral scans. The argon pulse shown in Fig. 20 was obtained by combining the intensities of the Ar^{+} and Ar^{++} fragments. From the ratio of the integrated pulses in Figs. 20 and 18, argon was found to be 98% of the residual gas in the 40-W TWT.

A second example is taken from the results of the analysis of a 10-W TWT. Figure 21 shows the total ions pulse and Fig. 22 shows the mass spectrum from one of the relevant spectral scans. The mass spectrum shows that methane is the predominant gas, with smaller amounts of argon, hydrogen, nitrogen, or carbon monoxide. The ion fragments from methane have been combined to give the pulse shown in Fig. 23. The ratio of the integrated pulses of Figs. 23 and 21 equates to 79% methane. Similar computations with the pulses from the ions corresponding to masses 2, 40, and 28 lead to 3% hydrogen, 8% argon, and 9% nitrogen or carbon monoxide, or a combination of both.

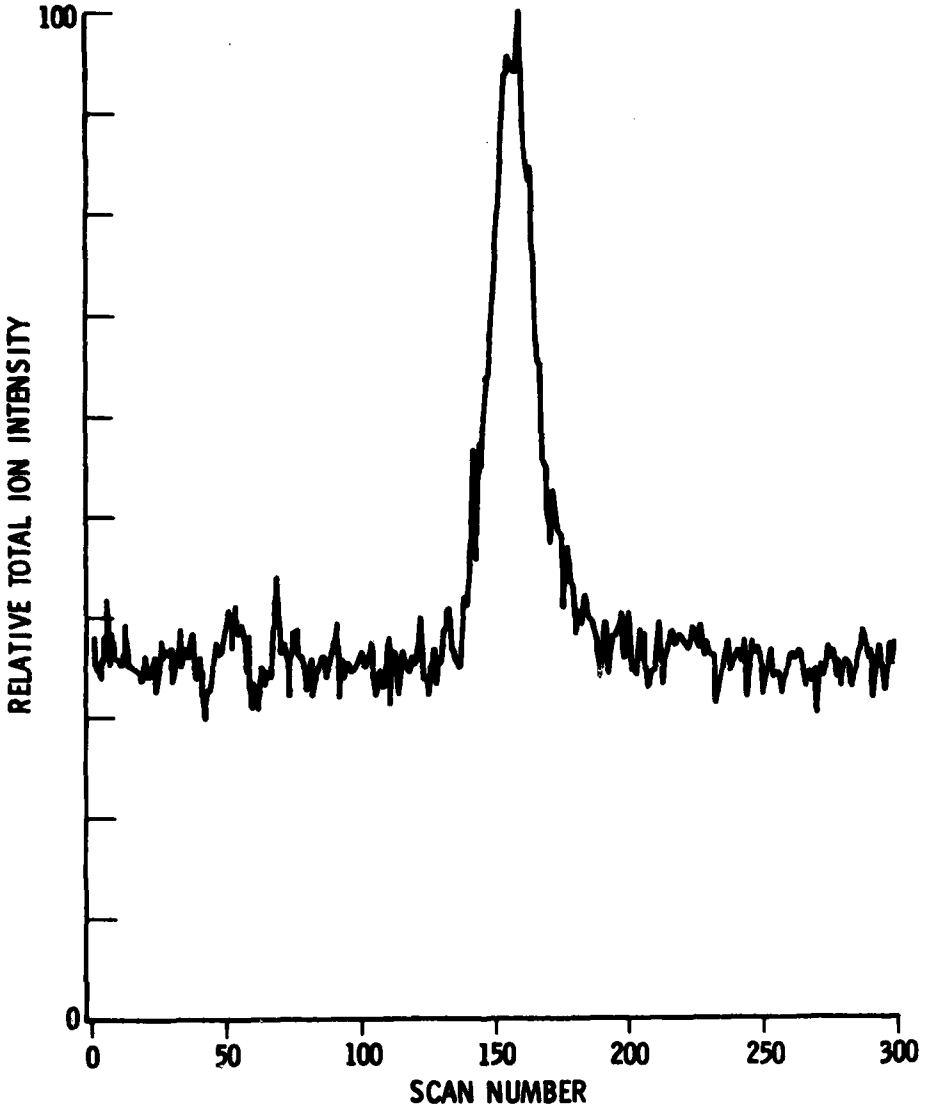

Fig. 18. Residual Gas Analysis of 40-W TWT: Total Ions Pulse from Repetitive Scanning of Mass Range during Sample Introduction

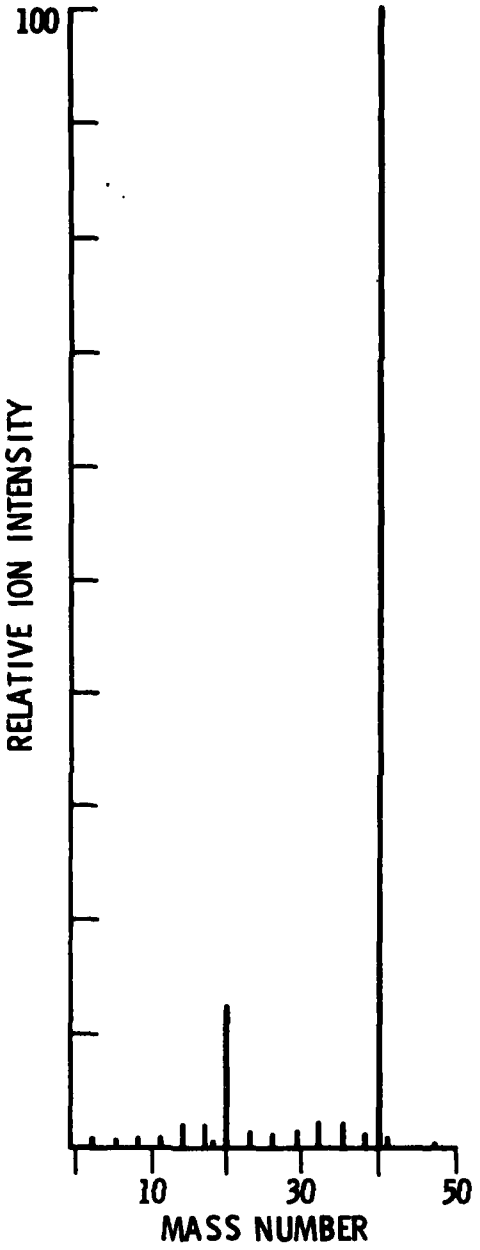

Fig. 19. Residual Gas Analysis of 40-W TWT: Mass Spectrum from Scan No. 156 after Background Correction

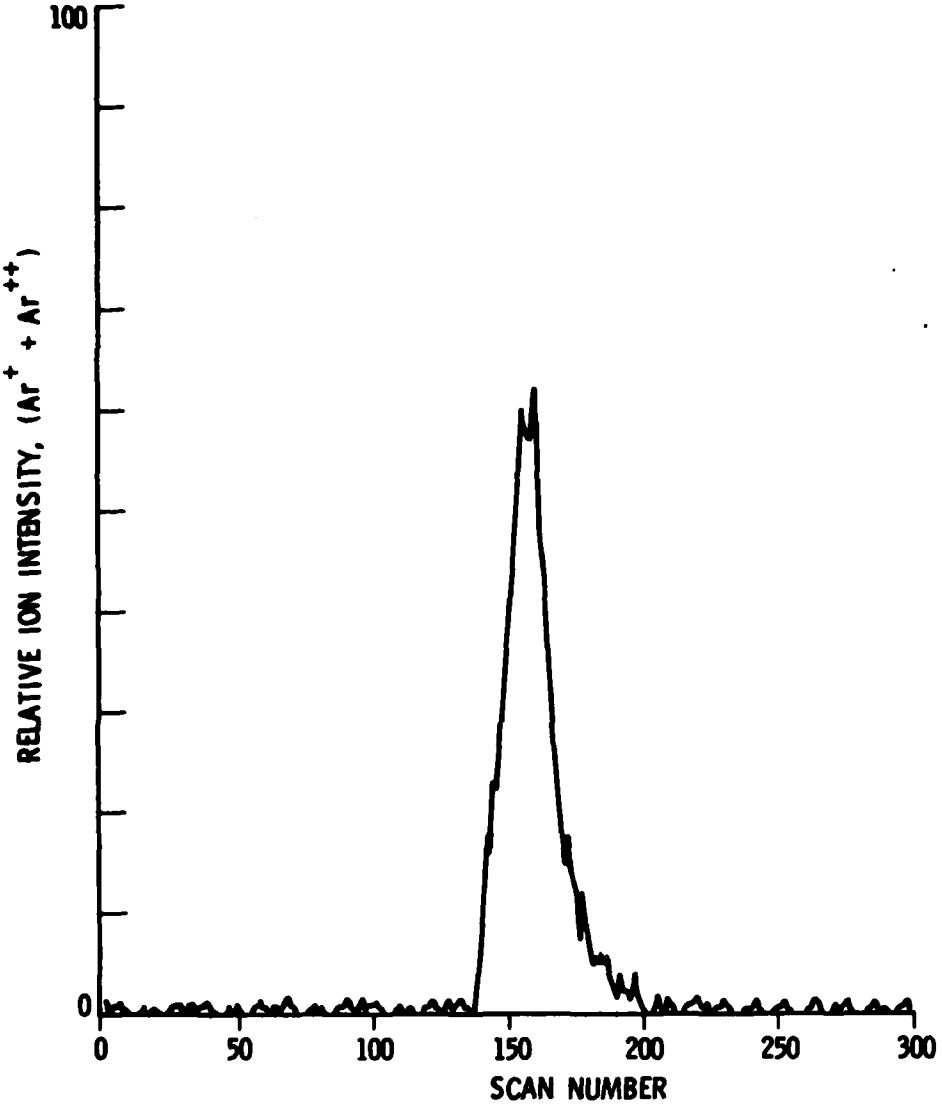

Fig. 20. Residual Gas Analysis of 40-W TWT: Argon Pulse from Repetitive Scanning during Sample Introduction

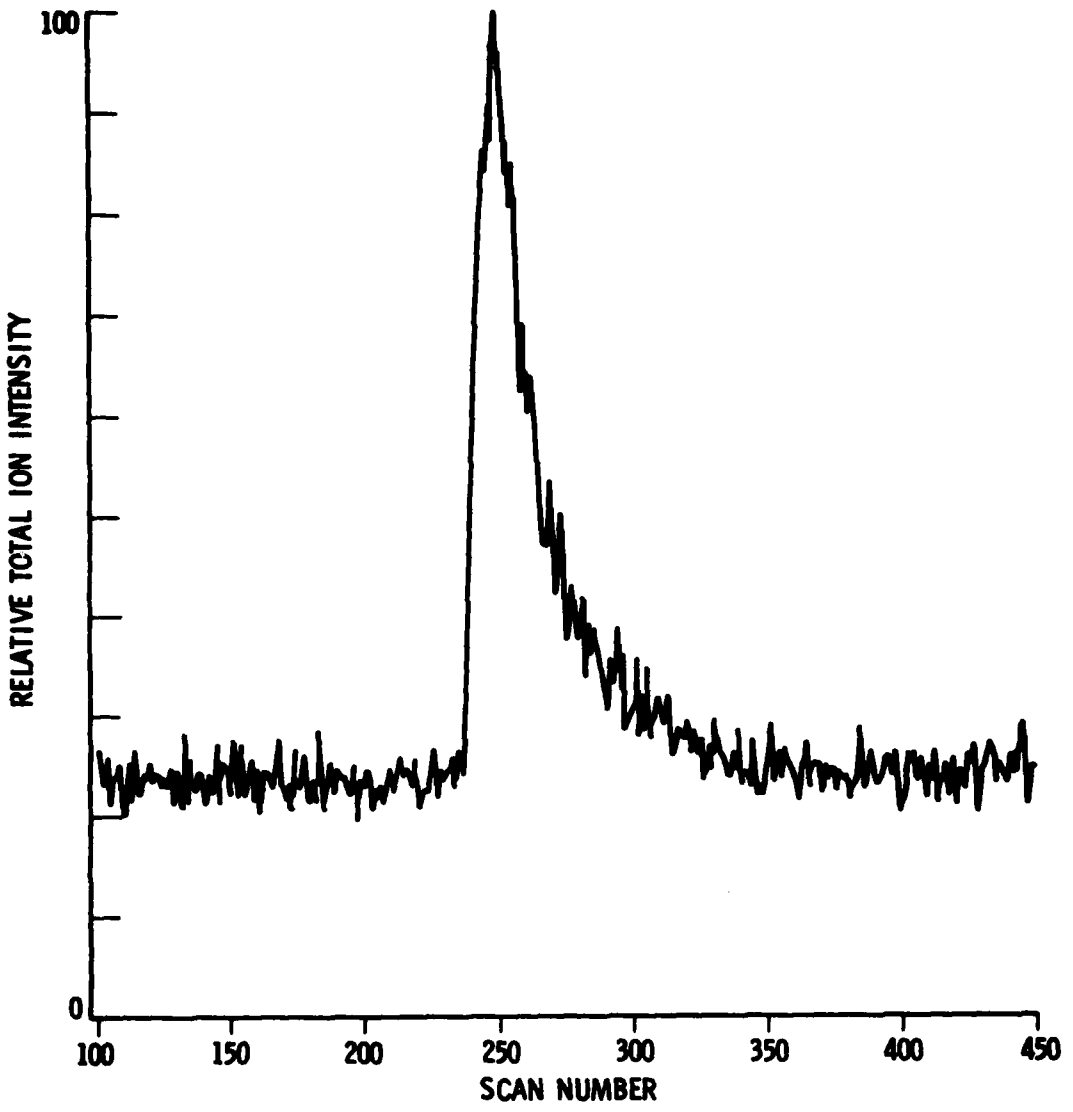

Fig. 21. Residual Gas Analysis of 10-W TWT: Total Ions Pulse from Repetitive Scanning of Mass Range during Sample Introduction

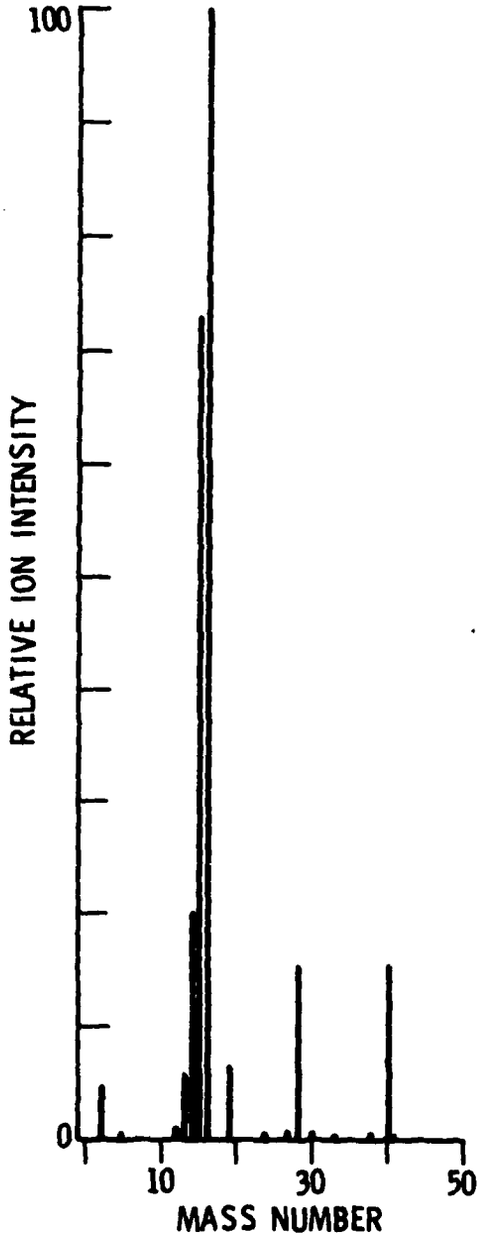

Fig. 22. Residual Gas Analysis of 10-W TWT: Mass Spectrum from Scan No. 248 after Background Correction

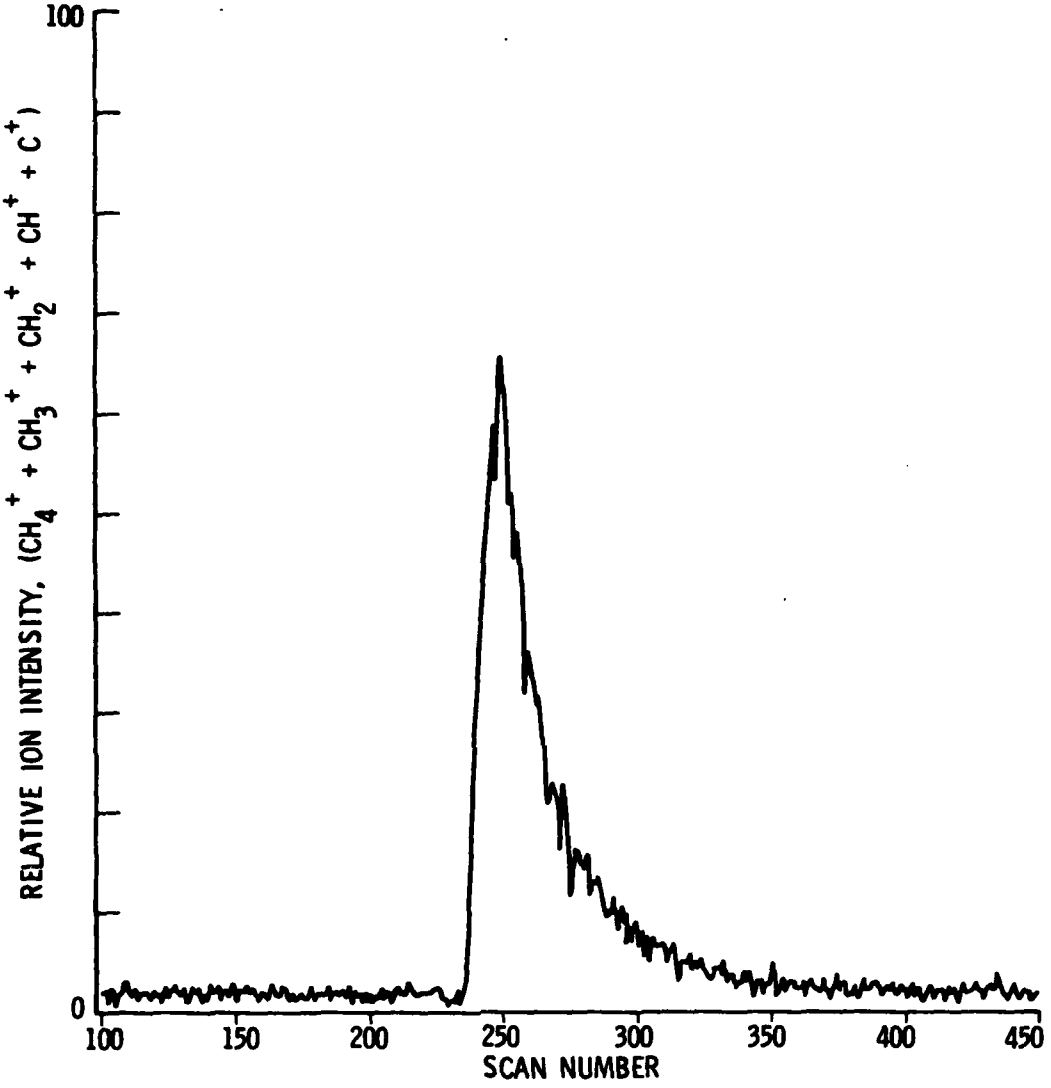

Fig. 23. Residual Gas Analysis of 10-W TWT: Methane Pulse from Repetitive Scanning during Sample Introduction

Although other analyses could be cited to illustrate various techniques that were employed, one final example will be given to show the versatility of the analytical method. A miniature lamp with an internal volume of only 0.025 cm^3 was subjected to residual gas analysis to determine its gas pressure and composition. The results of a control analysis with a blank lamp bulb showed that no detectable amount of gas was produced by fracturing the bulb in a preconditioned vacuum chamber. It was estimated that gas would have been detected if the gas pressure in a genuine lamp had been as low as 10^{-5} Torr. However, the results of analyzing two lamps showed that the actual gas pressures were more than 100-fold higher.

The last example exemplifies one of the formidable problems associated with the type of residual gas analysis that has been described. When a device is to be analyzed, one must be prepared to analyze a minimum detectable amount of gas while still being able to cope with an amount of gas that may be larger by several orders of magnitude. As the results in this report have demonstrated, the range of applicability of the dynamic method of analysis is more than adequate to meet this challenge.

REFERENCES

1. W. D. Davis, Trans. Tenth Nat. Vac. Symp., G. H. Bancroft, ed. (Macmillan Co., New York, 1963), p. 253.

2. H. Hintenberger, Ann. Rev. Nuclear Sci. 12, 435 (1962).

3. G. Lewin, Fundamentals of Vacuum Science and Technology (McGraw-Hill, New York, 1965), p. 95.

4. A. Guthrie, Vacuum Technology (John Wiley, New York, 1963), p. 173.

5. W. D. Davis, Trans. Ninth Nat. Vac. Symp., G. H. Bancroft, ed. (Macmillan Co., New York, 1962), p. 363.

6. J. R. Young and F. P. Hession, Trans. Tenth Nat. Vac. Symp., G. H. Bancroft, ed. (Macmillan Co., New York, 1963), p. 234.

7. H. Kobayashi, Trans. Tenth Nat. Vac. Symp., G. H. Bancroft, ed. (Macmillan Co., New York, 1963), p. 287.

LABORATORY OPERATIONS

The Laboratory Operations of The Aerospace Corporation is conducting experimental and theoretical investigations necessary for the evaluation and application of scientific advances to new military space systems. Versatility and flexibility have been developed to a high degree by the laboratory personnel in dealing with the many problems encountered in the nation's rapidly developing space systems. Expertise in the latest scientific developments is vital to the accomplishment of tasks related to these problems. The laboratories that contribute to this research are:

Aerophysics Laboratory: Launch vehicle and reentry aerodynamics and heat transfer, propulsion chemistry and fluid mechanics, structural mechanics, flight dynamics; high-temperature thermomechanics, gas kinetics and radiation; research in environmental chemistry and contamination; cw and pulsed chemical laser development including chemical kinetics, spectroscopy, optical resonators and beam pointing, atmospheric propagation, laser effects and countermeasures.

Chemistry and Physics Laboratory: Atmospheric chemical reactions, atmospheric optics, light scattering, state-specific chemical reactions and radiation transport in rocket plumes, applied laser spectroscopy, laser chemistry, battery electrochemistry, space vacuum and radiation effects on materials, lubrication and surface phenomena, thermionic emission, photosensitive materials and detectors, atomic frequency standards, and bioenvironmental research and monitoring.

Electronics Research Laboratory: Microelectronics, GaAs low-noise and power devices, semiconductor lasers, electromagnetic and optical propagation phenomena, quantum electronics, laser communications, lidar, and electro-optics; communication sciences, applied electronics, semiconductor crystal and device physics, radiometric imaging; millimeter-wave and microwave technology.

Information Sciences Research Office: Program verification, program translation, performance-sensitive system design, distributed architectures for spaceborne computers, fault-tolerant computer systems, artificial intelligence, and microelectronics applications.

Materials Sciences Laboratory: Development of new materials: metal matrix composites, polymers, and new forms of carbon; component failure analysis and reliability; fracture mechanics and stress corrosion; evaluation of materials in space environment; materials performance in space transportation systems; analysis of systems vulnerability and survivability in enemy-induced environments.

Space Sciences Laboratory: Atmospheric and ionospheric physics, radiation from the atmosphere, density and composition of the upper atmosphere, aurorae and airglow; magnetospheric physics, cosmic rays, generation and propagation of plasma waves in the magnetosphere; solar physics, infrared astronomy; the effects of nuclear explosions, magnetic storms, and solar activity on the earth's atmosphere, ionosphere, and magnetosphere; the effects of optical, electromagnetic, and particulate radiations in space on space systems.

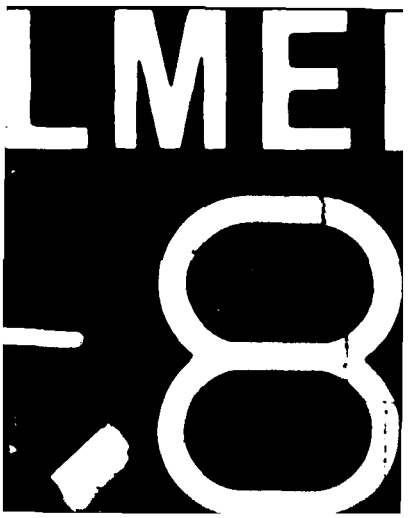
LME
.8